frontiers in Astronomy and Space Sciences

REVIEW
published: 24 September 2018
doi: 10.3389/fspas.2018.00032

Solar Physics From Unconventional Viewpoints

Sarah E. Gibson[1]*, Angelos Vourlidas[2], Donald M. Hassler[3], Laurel A. Rachmeler[4], Michael J. Thompson[1], Jeffrey Newmark[5], Marco Velli[6], Alan Title[7] and Scott W. McIntosh[1]

[1] High Altitude Observatory, National Center for Atmospheric Research , Boulder, CO, United States, [2] Applied Research Laboratory, Johns Hopkins University, Laurel, MD, United States, [3] Space Science and Engineering Division, Southwest Research Institute, Boulder, CO, United States, [4] NASA Marshall Space Flight Center, Huntsville, AL, United States, [5] NASA Goddard Space Flight Center, Greenbelt, MD, United States, [6] Earth, Planetary, and Space Sciences, University of California, Los Angeles, Los Angeles, CA, United States, [7] Lockheed Martin Solar and Astrophysics Laboratory, Palo Alto, CA, United States

We explore new opportunities for solar physics that could be realized by future missions providing sustained observations from vantage points away from the Sun-Earth line. These include observations from the far side of the Sun, at high latitudes including over the solar poles, or from near-quadrature angles relative to the Earth (e.g., the Sun-Earth L4 and L5 Lagrangian points). Such observations fill known holes in our scientific understanding of the three-dimensional, time-evolving Sun and heliosphere, and have the potential to open new frontiers through discoveries enabled by novel viewpoints.

Keywords: Sun, solar interior, photosphere, chromosphere, corona, heliosphere, space weather

Edited by:
Martin Anthony Hendry, University of Glasgow, United Kingdom

Reviewed by:
Vyacheslav Ivanovich Dokuchaev, Institute for Nuclear Research (RAS), Russia
CS Unnikrishnan, Tata Institute of Fundamental Research, India
Hugh Hudson, Space Sciences Laboratory, UC Berkeley, United States

Correspondence:
Sarah E. Gibson
sgibson@ucar.edu

Specialty section:
This article was submitted to Stellar and Solar Physics, a section of the journal Frontiers in Astronomy and Space Sciences

Received: *23 May 2018*
Accepted: *22 August 2018*
Published: *24 September 2018*

Citation:
Gibson SE, Vourlidas A, Hassler DM, Rachmeler LA, Thompson MJ, Newmark J, Velli M, Title A and McIntosh SW (2018) Solar Physics From Unconventional Viewpoints. Front. Astron. Space Sci. 5:32. doi: 10.3389/fspas.2018.00032

1. INTRODUCTION

Observations from satellite missions have transformed the field of solar physics. High-resolution observations with near-continuous temporal coverage have greatly extended our capability for studying long-term and transient phenomena, and the opening of new regions of the solar spectrum has made detailed investigation of the solar atmosphere possible. However, to date most solar space-based missions have been restricted to an observational vantage in the vicinity of the Sun-Earth line (SEL), either in orbit around the Earth or from the Sun-Earth L1 Lagrangian point. As a result, observations from these satellites represent the same geometrical view of the Sun that is accessible from the Earth.

Understanding the interior structure of the Sun and the full development of solar activity would benefit greatly from fully three-dimensional monitoring of the solar surface, atmosphere, and heliosphere. On the one hand, simultaneous spacecraft observations from multiple vantage points allow studies of the deep interior structure of the sun via stereoscopic helioseismology; on the other, distributed observations reveal the complete evolution of activity complexes and enhance space-weather predictions dramatically.

In this paper we will present the rich variety of science that is enabled by multi-vantage observations. In section 2 we review past and present missions that have ventured away from the SEL. In section 3 we discuss the science enabled by extra-SEL vantages, including solar dynamo studies, solar atmospheric global connections, and solar wind evolution and transient interactions. In section 4 we discuss the benefits of multi-vantage observations for space-weather monitoring, both for the Earth and other planets, and in section 5 we consider the discovery space opened by new viewpoints. In section 6 we identify the remaining key gaps in our heliospheric great observatory related to extra-SEL observations, and discuss how these may be filled through future opportunities–including both planned near-term missions and game-changing missions for the next decade and beyond. Finally, in section 7 we present our conclusions.

2. EXTRA-SUN-EARTH-LINE OBSERVATIONS TO DATE

The first extra-SEL observations in the inner heliosphere were obtained by the two Helios spacecraft, launched in 1974 (Helios-1) and 1976 (Helios-2). This mission obtained primarily *in-situ* measurements of solar wind plasma and cosmic rays (Gurnett et al., 1975; McDonald et al., 1977; Rosenbauer et al., 1977), Faraday rotation measurements of light from external sources passing through the corona (e.g., Bird et al., 1985), as well as remote sensing observations (but no imaging) of interplanetary dust (Leinert et al., 1981) and coronal mass ejections (CMEs) (Jackson, 1985). The Helios spacecraft stayed close to the ecliptic plane; sample orbits are shown in **Figure 1** (Helios-2 has the current record for proximity to the Sun at 0.29 AU). Other extra-SEL, near-ecliptic *in-situ* solar wind measurements have been obtained by planetary missions, such as MESSENGER (Solomon et al., 2001), Pioneer Venus Orbiter (Colin, 1980), and the STEREO twin spacecraft (Kaiser et al., 2008), which precede and follow the Earth's orbit.

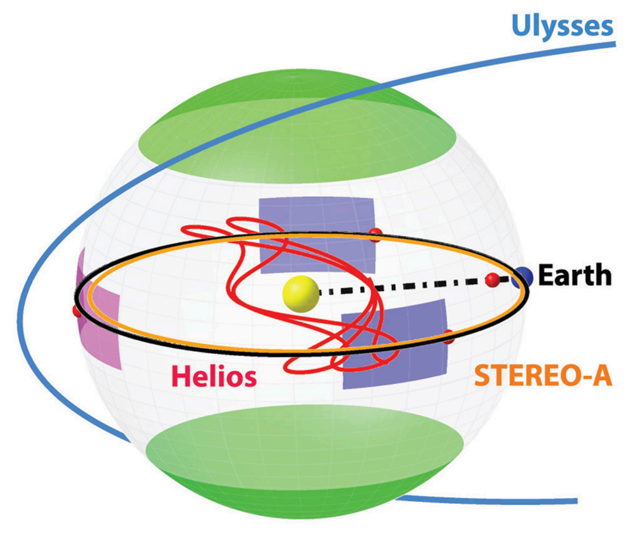

FIGURE 1 | An overview of interesting vantage points, highlighting previous extra-Sun-Earth-line (extra-SEL) missions. Sun and Earth are shown as yellow and blue dots, and Lagrange points are shown as red dots (radial scale deformed for clarity). The SEL is indicated as the black dot-dashed line (intersecting the L1 Lagrange point and Earth). The quadrature views are shown as blue patches (intersecting the L4 and L5 Lagrange points); the far-side view as a pink patch (intersecting the L3 Lagrange point); and the polar views as green patches. Sample STEREO orbit is shown in orange, Helios orbits in red, and Ulysses orbit in light blue. The Helios orbits are relative to the Earth, i.e., Heliocentric Earth Ecliptic (HEE) coordinates, the other orbits are in Heliocentric Inertial coordinates (Thompson, 2006).

The corona and inner heliosphere (defined here at the space within 1 AU of the Sun) have been observed through extra-SEL, near-ecliptic imaging only since 2006 when the Sun-Earth Connection Coronal and Heliospheric Investigation (SECCHI) (Howard et al., 2008), comprising an EUV imager (EUVI), two coronagraphs (COR1-2), and two heliospheric imagers (HI1, HI2), was deployed aboard both STEREO spacecraft (sample STEREO-A orbit is shown in **Figure 1**).

Since separating beyond $\approx 20^\circ$ from Earth in early 2008, STEREO began partial imaging of the far-side EUV corona. In 2011, the STEREO reached opposition and achieved the first "synchronic" observation of the full 360° corona (**Figure 2**; see also section 3.2). Although STEREO did not carry any magnetographic capability, its 360° coverage has enabled some degree of validation for flux transport models (Ugarte-Urra et al., 2015) and helioseismic predictions of far-side flux emergence (Liewer et al., 2017). As of 2018, STEREO-A continues to image the far-side and provide, with the support of SDO/AIA observations, instantaneous coverage of more that two-thirds of the corona.

Prior to STEREO, Earth-directed solar wind properties were generally derived indirectly by modeling and were validated by *in-situ* measurements. The sparseness of inner heliospheric measurements considerably hindered the study of large-scale solar-wind structures, including stream-stream interaction regions—or corotating interaction regions (CIRs) in their evolved form—and interactions among CMEs or between CMEs and the ambient solar wind. The continuously varying extra-SEL STEREO viewpoints have opened up research in many, previously elusive areas: from EUV coronal stereoscopy (Aschwanden, 2011) and limb observations of the origins of Earth-directed CMEs (e.g., Patsourakos et al., 2016) to CIRs, CMEs entrained in CIRs (Rouillard et al., 2009), and interacting CMEs (Sheeley et al., 2008; Lugaz et al., 2017). The primary objective of the STEREO, driving its multi-viewpoint mission design, was to discover the 3D structure of CMEs. The power of this approach to recover CME sizes, directions, and detailed kinematics has been demonstrated by many studies (e.g., Thernisien et al., 2009; Bosman et al., 2012; Sachdeva et al., 2017, to name a few).

The only spacecraft to explore the heliosphere outside of the ecliptic plane was Ulysses (1990–2009), which achieved a high-inclination (80°) near-polar orbit with a Jupiter swing-by. Ulysses measured the solar wind plasma, electromagnetic fields, and composition *in situ* in the distance range between 1.3 and 5.4 AU from the Sun (Bame et al., 1992; Balogh et al., 1992; Gloeckler et al., 1999). Ulysses confirmed that the global, three-dimensional structure of the solar wind around solar minimum is made up of a fast, uniform flow in the northern and solar polar regions, and slow-to-medium speed wind streams originating in a coronal streamer belt that is confined to a relatively narrow range of latitudes on either side of the heliographic equator (McComas et al., 1998). This band, in which the majority of solar wind variability is observed to occupy some 43° in latitude, also contains the heliospheric current sheet (HCS) that separates the oppositely directed large-scale magnetic fields originating in the two hemispheres. During its second polar pass at solar

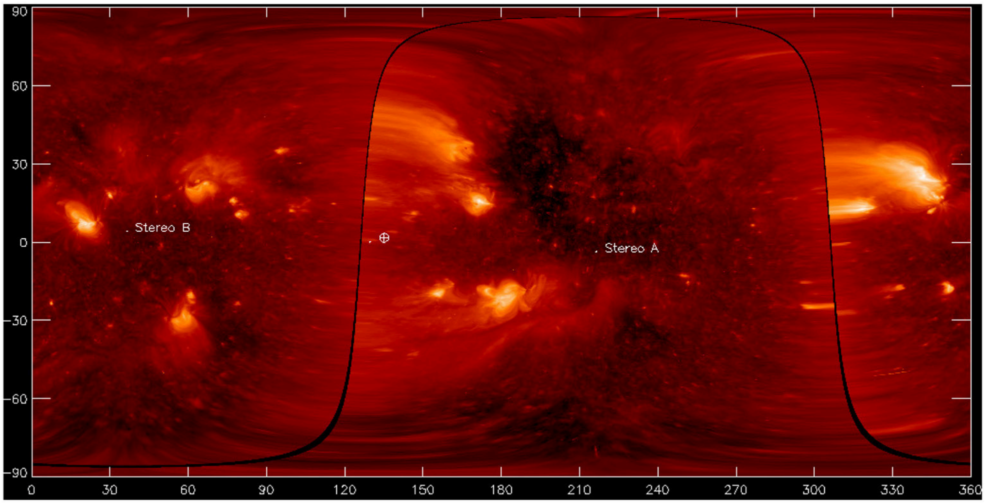

FIGURE 2 | A Carrington map of EUV synchronic observations of the full 360° sun, made possible by far-side imaging provided by the twin STEREO spacecraft. Images were taken in the 284 Å channel on February 6, 2011 at 18:00 UT while the STEREO spacecraft were in exact opposition.

maximum, Ulysses found a much more symmetric heliosphere with no systematic dependence on latitude (McComas et al., 2003). The wind itself was generally slower and much more variable than at solar minimum at all latitudes. During its third and final polar pass, Ulysses found that the very strong solar minimum of 2008 did not lead to slower winds, but to a less dense wind (around 20%) and lower momentum flux, while continuing to exhibit a generally dipolar structure (Issautier et al., 2008). Ulysses also carried an X-ray/cosmic ray burst instrument (GRB) (Hurley et al., 1992) that was used in conjunction with measurements from the Hard-Xray telescope on the Yohkoh satellite (Kosugi et al., 1991) for stereoscopic analysis of solar flares (Kane et al., 1998). Unfortunately Ulysses did not carry a Doppler magnetograph, so the details of solar polar flows and magnetic fields, and the weakening of the magnetic field over the last solar cycles, remain largely mysterious to this day.

3. SCIENCE ENABLED BY EXTRA-SUN-EARTH-LINE OBSERVATIONS

The scientific benefit of extra-SEL observations has been demonstrated to some extent by the missions described in section 2, but, in many cases, these observations merely whet our appetite for more comprehensive and sustained measurements. We now describe the science enabled by extra-SEL observations, and identify areas where new observations are most desired.

3.1. Solar Dynamo: Interior to Surface

While both the STEREO and Ulysses missions led to many scientific breakthroughs, there is no doubt that the lack of Doppler magnetographs on these extra-SEL spacecraft was a missed scientific opportunity. In addition to providing critical information about the surface magnetic field distribution and Doppler flow fields, these observations are the key inputs to helioseismic inversions. The power of helioseismology for probing the interior of the Sun has been proven by observations from views along the Sun-Earth line (Christensen-Dalsgaard, 2002; Basu and Antia, 2008), using both ground-based (e.g., Elsworth et al., 1994; Harvey et al., 1996) and space-based (e.g. Gabriel et al., 1997; Kosovichev et al., 1997) observing platforms.

In particular, global helioseismology, which studies the Sun's resonant modes manifesting as solar surface oscillations, revealed the Sun's internal structure and rotation as never before. The "tachocline," a boundary layer between the rigidly-rotating core and differentially-rotating convective envelope was deduced, and the variation of this differential rotation with latitude and depth probed (Thompson et al., 2003; Christensen-Dalsgaard and Thompson, 2007).

By observing wave packets rather than resonant modes, local helioseismology provides another tool for imaging the time-varying structure and flows for local areas of the Sun (Gizon et al., 2010). For example, ring-diagram analysis measures distortions of the power spectrum of acoustic wave fields due to flows (Hill, 1988; Schou and Bogart, 1998). Time-distance analysis (Duvall et al., 1993; Kosovichev, 1996) determines sub-surface structure and flows by examining correlations between different points on the surface: note that both ends of a ray path must be resolved, so that single-vantage observations are necessarily limited to shallow waves and thus near-surface structures. Finally, holography infers sub-surface inhomogeneities from perturbations of the acoustic wave field, and has been used to examine structure below sunspots as well as the emergence of active regions on the far side of the Sun (Lindsey and Braun, 1997; Chang et al., 1997). In contrast with global helioseismology, local helioseismology has the power to study how the solar structure and dynamics vary with longitude, and to distinguish differences between the northern and southern hemispheres.

In addition to helioseismology, observations of surface Doppler velocities and correlation tracking of magnetic features have been used to study meridional circulation, torsional oscillations, and supergranule patterns (Howe, 2009; Rieutord and Rincon, 2010). These, along with observations of magnetic flux emergence over solar-cycle time scales provide inputs to surface-flux-transport and dynamo models (Mackay and Yeates, 2012).

Despite the strides made over the past two decades, important open questions about solar interior structure and flows remain. Helioseismology and photospheric measurements have provided a tantalizing glimpse of multi-cell flow patterns, with variation in both radius and latitude; however, different methods have given different results (Hanasoge et al., 2015). In particular, because of the geometric limitations of the SEL vantage, there is uncertainty about the polar structure and flows, and about the strength and distribution of polar magnetic fields.

These represent critical observational constraints on solar dynamo models. They are particularly significant to the popular Babcock-Leighton/flux transport dynamo paradigm, as the cyclic reversals of polar fields in those models is sensitive to the structure of the high-latitude meridional flow, and to the magnetic flux budget associated with the transport and evolution of magnetic fields over the solar cycle (Charbonneau, 2010; Hathaway, 2015). They also are relevant to understanding the fundamental physics of convection and its role in the dynamo. For example, observations from multiple vantages may reveal important differences in the structure and transport between polar and equatorial convective modes that determine global mean flow properties (Miesch, 2005) (see also discussion in section 5 regarding polar complexities ripe for discovery).

Extra-SEL observations complement existing SEL observations in multiple ways (**Table 1**). Multiple views increase surface coverage and help with disentangling different modes, improving signal-to-noise for both global and local helioseismic methods. They enable time-distance analysis of longer ray paths, probing deeper below the solar surface to resolve large-scale convection, giant cells, and possibly even the tachocline itself. Moving away from the SEL provides longitudinal coverage, yielding a more complete view of surface flow patterns and a comprehensive view of magnetic flux emergence and evolution. Finally, observing from higher latitudes gives a direct view of polar fields and flows, and breaks north-south symmetries. To make progress on the open questions on the solar dynamo, extra-SEL observations are needed to resolve solar surface-to-interior flows and magnetic fields as a function of longitude, latitude, and depth, and over the solar cycle. The polar vantage is particularly helpful because of the critical information on polar fields and flows that it provides.

3.2. Solar Atmosphere: Global Connections

In addition to providing an upper boundary on the solar interior, Doppler magnetographs of the photosphere provide the lower boundary on the heliosphere. Global models, ranging from potential-field-source-surface extrapolations (e.g., Wang and Sheeley, 1990; Arge et al., 2003) to magnetohydrodynamic simulations (e.g., Tóth et al., 2005; Riley et al., 2012) use photospheric observations to simulate the magnetic fields of the solar corona and heliosphere.

The single SEL vantage is a significant limitation, however. Foreshortening affects both the poles and the East/West limbs. Magnetic fields on the far-side of the Sun are not seen at all, until they rotate into view. As a result, global magnetic boundary conditions on models cannot represent any single time, and indeed incorporate measurements taken over multiple days or even weeks. Standard synoptic maps are made up of an average in which each longitude is weighted toward observations taken when that longitude is at disk center (Hoeksema and Scherrer, 1986). Alternatively, "synchronic" methods weight the entire map toward a single time, making use of flux-transport models and data assimilation (Worden and Harvey, 2000; Schrijver and De Rosa, 2003; Arge et al., 2010; Hickmann et al., 2015). Multiple views clearly are of great benefit to providing a synchronic view, as was shown in **Figure 2** using EUV STEREO observations. They are also important for obtaining a complete picture of magnetic flux emergence: this is critical for CME studies, since most occur in the 24–48 h after new flux emerges. The addition of magnetograph measurements from a quadrature (L5) viewpoint is expected to significantly improve global magnetic simulations (Mackay et al., 2016), as well as to improve modeling of the heliosphere (Pevtsov et al., 2016).

Flux-transport models operating over solar-cycle time scales have also been used to model the evolution of polar magnetic fields. It is difficult to validate such models, however. Although the approximately seven-degree inclination of the Sun's rotational axis with respect to the ecliptic plane means that observations from the Earth catch a glimpse of each solar pole once per year, they are still viewed from a very large angle, making accurate measurements of the polar photospheric magnetic fields extremely difficult (Petrie and Low, 2005). Tsuneta et al. (2008) used high-resolution spectropolarimetric observations from the Solar Optical Telescope on board

TABLE 1 | Solar interior and dynamo studies enabled by extra-SEL observations.

Open science questions	What are the solar surface/interior flow and magnetic field patterns vs. longitude, latitude, and depth, and how do they constrain dynamo models?			
Measurements needed	(1) Full-disk Doppler vector magnetographs (photosphere)			
Benefits from extra-SEL vantage (assumes existence of complementary SEL observations)		**Polar**	**Quadrature**	**Far-side**
	Helioseismic inversions able to probe deeper	Yes (1)	Yes (1)	Yes (1)
	Comprehensive view of flux emergence and evolution	Yes (1)	Yes (1)	Yes (1)
	Polar fields and flows directly observed; North-South symmetry broken	Yes (1)	No	No

Hinode to resolve magnetic structures at the poles during a time of maximum polar inclination relative to the Earth, finding concentrated patches of strong field. A comparison of the average magnetic flux implied by these high-resolution measurements to photospheric magnetic synoptic maps implies that the polar fields may be significantly underestimated, which could also explain inconsistencies with measurements of the open magnetic flux in the heliosphere (Linker et al., 2017).

In general, there remain substantial uncertainties about the photospheric magnetic boundary (Riley et al., 2014). This affects not just global models but also magnetic models of particular coronal structures (e.g., active regions, prominences...) that are also sensitive to uncertainty in the magnetic boundaries (De Rosa et al., 2009). In addition to center-to-limb foreshortening issues, vector magnetic measurements from a single viewpoint possess intrinsic ambiguities (Semel and Skumanich, 1998). These hamper our ability to determine the three-dimensional coronal magnetic field, and hence to investigate the roles of stored magnetic energy, magnetic helicity, and topology in solar eruptions. Coronal plasma and polarimetric measurements can be used to address such limitations by providing independent measurements for validation and/or optimization of coronal magnetic models (Savcheva et al., 2014; Malanushenko et al., 2014; Gibson et al., 2016).

The optically-thin corona is under-resolved by a single line of sight; multiple vantages enable more comprehensive tomographic and/or stereoscopic methods (see e.g., Aschwanden, 2011 and references therein). Such methods are useful for characterizing the morphology and spatial variation of the coronal density, temperature, and magnetic field (see e.g., Vasquez et al., 2011; Aschwanden et al., 2015; Kramar et al., 2016). Stereoscopy is also a powerful tool for distinguishing between models of flare acceleration and collisional and non-collisional transport processes (Casadei et al., 2017).

Modeling coronal structures observed at the limb is also fundamentally limited by the fact that observations of the underlying on-disk magnetic boundary cannot be co-temporal, whereas observations from the pole or quadrature enable simultaneous study of limb and disk. This is particularly valuable for analyzing source regions of the solar wind using multiwavelength spectroscopy: both limb and disk observations are used to quantify the properties at the corona, and then the science is maximized via complementary *in-situ* solar-wind observations (including composition measurements). These include both solar wind transient structures and the ambient solar wind from coronal holes. Since EUV and UV spectrographs can only measure line-of-sight velocities, previous observations of the solar wind outflow in polar coronal holes with the SUMER spectrograph on SOHO (Hassler et al., 1999; **Figure 3**) have been limited at the poles. A polar mission could achieve direct measurements–both on-disk and *in-situ*–that explore fast solar wind sources and related structures, such as polar plumes associated with polar coronal holes (Deforest et al., 1997; Hassler et al., 1997), free from the effects of the foreshortening that has been inherent in observations to date (McIntosh et al., 2006).

Not only are there open questions about the global heliosphere and the localized coronal magnetic structures that are solar-wind

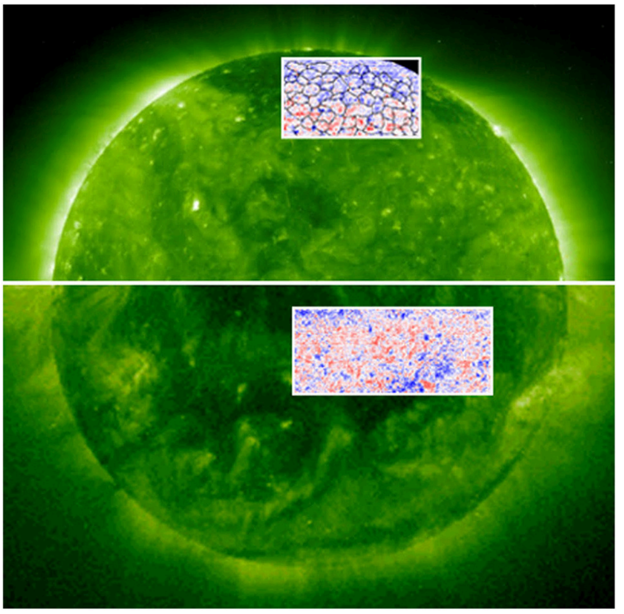

FIGURE 3 | Line-of-sight velocity structures observed by the SUMER instrument on SOHO show correlation of outflow velocity with chromospheric network structure within coronal holes both at mid-latitudes **(bottom)** and at high latitudes **(top)** (Hassler et al., 1999). As can be seen in the figure, observations of the detailed structure of solar wind outflow at the poles is made difficult by foreshortening, and would be significantly improved by out-of-the-ecliptic observations.

source regions, but there are also questions about the nature of interactions between such local and global magnetic fields. One of the most tantalizing findings of multi-viewpoint imaging is the evidence for long-range interactions between eruptive events occurring over the span of days across a full solar hemisphere (Schrijver and Title, 2011; Titov et al., 2012, 2017). While the subject of "sympathetic" flaring and remote triggering of flares or eruptions has been discussed for decades in the literature, it can not be unambiguously resolved without synoptic 360° coverage of the corona. Similarly, large-scale waves associated with eruptions often have global properties that require longitudinal coverage (e.g., Thompson and Myers, 2009; Olmedo et al., 2012).

Extra-SEL observations thus complement existing SEL observations in multiple ways (**Table 2**). They improve coverage of the boundary of the heliosphere and of the birth-to-death evolution of solar structures, including global interactions. More viewpoints also help vector magnetic field disambiguation and model optimization/validation, as well as stereoscopic/tomographic reconstructions of 3D coronal magnetic fields, thus yielding key information about magnetic energy, helicity, and topology. Finally, simultaneous observations of structures at the limb and of the boundary beneath them allows comprehensive studies of the coronal structures that are the source of the solar wind. To make progress on the open questions on the global connections of the solar atmosphere, extra-SEL observations are needed for better coverage and

TABLE 2 | Solar atmosphere/global connections studies enabled by extra-SEL observations.

Open science questions	What is the structure of the global coronal/heliospheric magnetic field? What are the source regions of the solar wind? How is magnetic energy stored/released in eruption, and what is role of helicity/topology? How do local and global solar magnetic fields interact?			
Measurements needed	(1) Full-disk Doppler vector magnetographs (photosphere) (2) Chromospheric spectropolarimeters (3) Full-Sun multiwavelength coronal imagers (4) Multiwavelength coronal spectrometers (5) Polarimetric coronagraphs (6) White-light/multiwavelength coronagraphs (7) Heliographic imagers (HIs) with polarizers (8) *In-situ* solar wind measurements			
Benefits from extra-SEL vantage (assumes existence of complementary SEL observations)		**Polar**	**Quadrature**	**Far-side**
	Better coverage of global magnetic boundary; *Better constraints on contribution of polar fields to heliospheric open flux	Yes* (1; 8)	Yes (1)	Yes (1)
	Magnetic vector boundary 180° disambiguation	Yes (1–2)	Yes (1–2)	No
	More cotemporal lines of sight to reconstruct 3D coronal structures	Yes (3–6)	Yes (3–6)	No
	Boundary/limb view of structures observed simultaneously; solar-wind source regions connected to *in-situ* measurements; global interactions comprehensively observed	Yes (1–8)	Yes (1– 8)	No

disambiguation of the vector magnetic boundary and for multi-vantage observations of optically-thin structures. The polar vantage is particularly important to resolve uncertainty in the magnetic boundary condition and solar-wind source regions at high latitudes, with implications for the open magnetic flux in the heliosphere.

3.3. Solar Wind and Transients: Evolution and Interactions

As discussed in section 2, STEREO revolutionized heliospheric physics by providing consistent, spatially resolved imaging of the inner heliosphere with coverage from the Sun to 1 AU. When viewing from the extra-SEL, the STEREO heliospheric imagers can observe CIRs and CMEs en route to Earth without interruption (**Figure 4**), enabling studies of their evolution and interactions, and naturally feeding an increasingly sophisticated space-weather research field (see further discussion in section 4).

While the STEREO mission demonstrates that we can indeed image the solar wind and its major components, it has left us with many unanswered questions. With regards to CMEs, heliospheric imaging analyses provide some indications of CME rotational evolution en route to Earth (e.g., Isavnin et al., 2014) and multiple cases of CME-CME interactions (Lugaz et al., 2017, and references therein), but it is hard to establish the reliability and general applicability of these results due to the long integration times and low spatial resolution of the current imagers on STEREO. Projection effects, long lines of sight through overlapping structures, and potentially complex internal morphology complicate the interpretation. Evolutionary effects such as ambient plasma pileup can also modify the brightness distribution around the transient, and skew triangulation or 3D reconstruction results. This is particularly relevant to longitudinal deflections (Wang et al., 2004; Isavnin et al., 2014), as their study relies almost exclusively on imaging analysis. Extra-SEL/SEL coronagraph and heliospheric imagers are needed with better sensitivity, and with polarization capabilities to localize plasma in 3D (DeForest et al., 2016). For maximum scientific return these need to be coupled with the complementary SEL/extra-SEL *in-situ* measurements during CME-CME (or equally, CME-CIR) interactions.

Existing observations of the corona and inner heliosphere have also provided us with tantalizing clues that the laminar flow of the slow solar wind, revealed by the familiar streamer structure in coronagraph images, breaks into a more turbulent flow beyond 15–20 Rs (DeForest et al., 2014). This is the height range where the wind may become super-Alfvénic, according to models (Verdini et al., 2009; Katsikas et al., 2010; Zhao and Hoeksema, 2010; Goelzer et al., 2014; Tasnim and Cairns, 2016). This is also the height, however, where current observations transition from a coronagraph to a heliospheric imager with lower spatial resolution and longer integration times. It is, therefore, unclear whether the change in the solar wind appearance is due to instrumental limitations or reflects a true change in the nature of the solar wind. *In-situ* measurements of the interplanetary magnetic field (IMF) in the corona, soon to be provided by the Parker Solar Probe (Fox et al., 2016) (section 6.1), will go a long way toward answering this issue. This will be done, however, over relatively limited spatial and temporal ranges.

Extra-SEL heliospheric observations complement existing SEL observations in multiple ways (**Table 3**). Both polar and quadrature viewpoints allow imaging of Earth-intersecting transient structures, and also permit *in-situ* measurements of structures imaged from the SEL. In so doing they shed light on the nature of solar-wind/transient interactions, and enable important

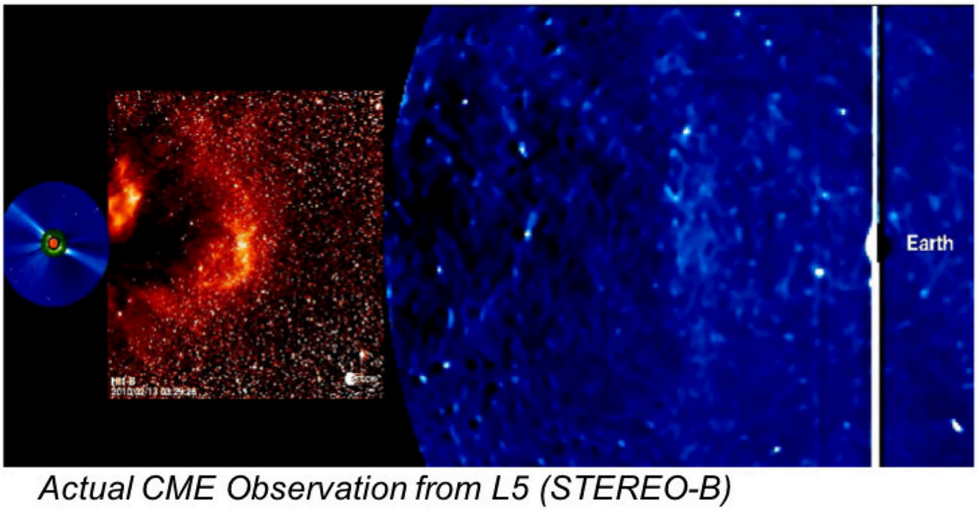

FIGURE 4 | Snapshot of an Earth-directed CME from the STEREO-Behind imagers while crossing the L5 point (02/13/2010 3:29 UT). The figure is a composite of the fields of view (FOVs) of all SECCHI imagers. The CME is in the HI1-B FOV at this time. The Earth is bright and saturates a few columns in the HI2-B FOV. The faint broad front of a preceding CME can be discerned in HI2-B.

TABLE 3 | Solar-wind/heliospheric transient studies enabled by extra-SEL observations.

Open science questions	How do transients evolve and interact with the ambient solar wind as they move through the heliosphere?			
Measurements needed	(6) White-light/multiwavelength coronagraphs (7) Heliographic imagers (HIs) with polarizers (8) *In-situ* solar wind measurements			
Benefits from extra-SEL vantage (assumes existence of complementary SEL observations)		**Polar**	**Quadrature**	**Far-side**
	More lines of sight to reconstruct 3D solar-wind structures	Yes (6; 7)	Yes (6–7)	No
	Complementary *in-situ* probing and remote imaging of solar wind/transient evolution	Yes (7–8)	Yes (7–8)	No
	Longitudinal structure of Alfvén surface and of CMEs, CIRs, and shocks revealed	Yes (6–7)	No	No

monitoring of space weather (see section 4). Capturing the large scale structure of the Alfvénic surface and its interplay with the outflowing solar plasma in a synoptic manner particularly benefits from the polar viewpoint. This viewpoint, unavailable even to the Solar Orbiter mission which will only reach 34° above the ecliptic (Müller et al., 2013) (section 6.1), comprehensively reveals both the radial and longitudinal evolution of the solar wind and transient structures propagating through it (**Figure 5**). It is particularly good for capturing the formation and evolution of CIRs and shocks in a continuous fashion and for investigating the magnetic connectivity across large swaths of space. To make progress on the open questions on CME/CIR propagation, their interactions and the role and nature of the ambient solar wind, we need spatially resolved coverage of the inner heliosphere–both *in-situ* and (critically) imaging–at temporal scales matching the evolutionary timescales of these phenomena (tens of minutes to hours), and from multiple vantage points. The polar vantage is particularly beneficial because of the wide coverage and unique perspective it provides.

4. SPACE-WEATHER SIGNIFICANCE OF EXTRA-SUN-EARTH-LINE OBSERVATIONS

In addition to all that may be gained scientifically from extra-SEL observations, there are clear benefits to such measurements for space-weather prediction and monitoring.

First of all, global coverage enables analysis of active longitudes (de Toma et al., 2000), which have been connected to particularly strong and sustained space-weather activity (Castenmiller et al., 1986; Bai, 1987; McIntosh et al., 2015). Similarly, longitudinal coverage is important for monitoring the development and evolution of long-lived low-latitude coronal holes, which can be the source of repeating high-speed solar wind streams that drive periodic geomagnetic, upper atmosphere, and radiation belt responses (Gibson et al., 2009). The benefits extend to irradiance measurements, which are limited near the solar limbs. Monitoring irradiance variations from a quadrature viewpoint would improve the short-term (7+ days) forecast accuracy of thermospheric and ionospheric density (Vourlidas,

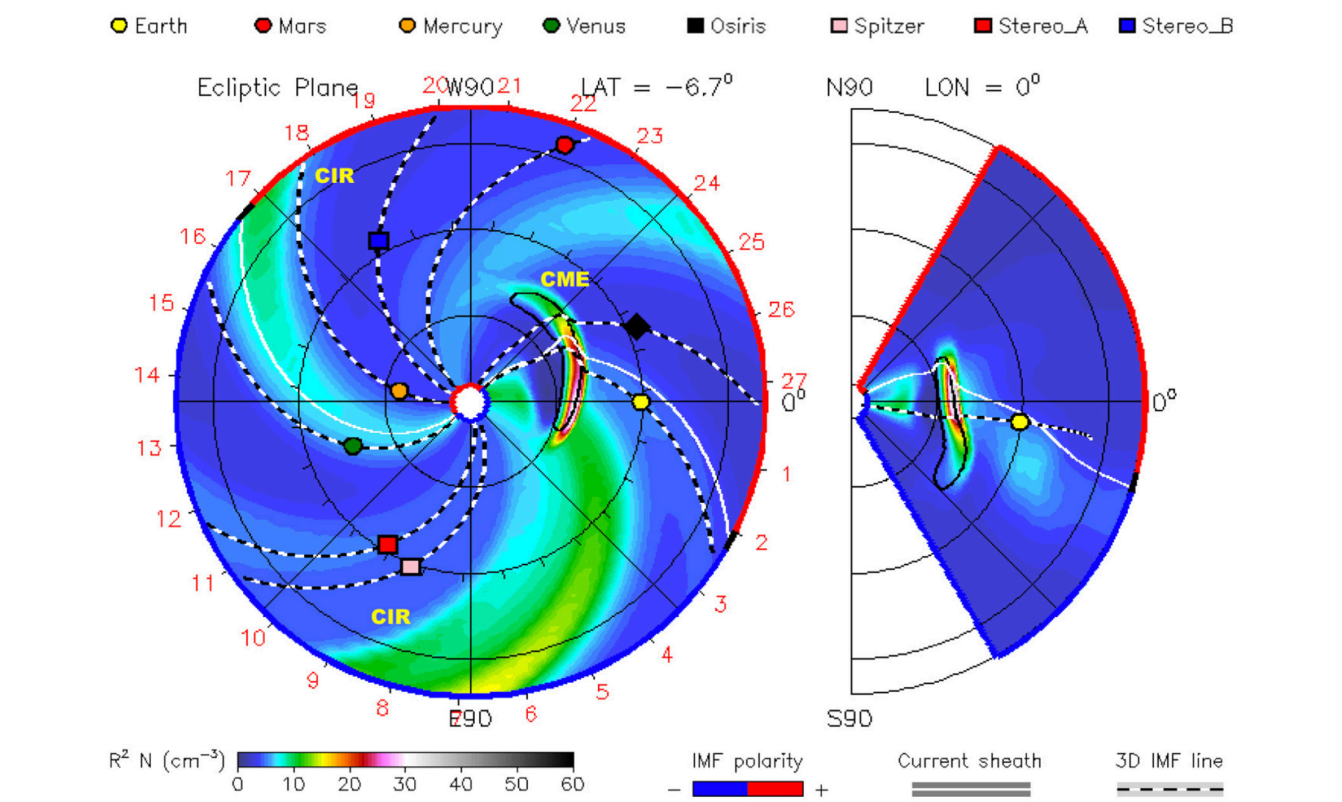

FIGURE 5 | Snapshot of the heliosphere, on 2/14/2018 00:00 UT, from an ENLIL model run at the Community Coordinated Modeling Center. The normalized density is shown. **(Left)** Polar view showing one CME and two CIRs. Earth is magnetically connected to the incoming CME. The interaction of the CME and a CIR is evident in this view. **(Right)** Meridional cut at the location of Earth. It approximates the view from a heliospheric imager in Earth quadrature.

2015), important for satellite collision avoidance analyses and military applications. The current 7+ day forecasts lie outside the acceptable range of many users, especially around the maximum of solar activity (Vourlidas, 2017). The additional benefits of irradiance measurements from a polar viewing spacecraft would be less significant, since most irradiance variation occurs at active region latitudes, which are still close to the limb of a polar viewer. However, see section 5 for discussion of discovery irradiance science from the polar vantage.

Beyond this, limb observations from the poles or quadrature provide a variety of information to improve space-weather forecasts. Before the eruption, these views enhance predictive capability for impending SEL-directed CMEs. For example, the presence of a tear-drop morphology in coronal cavities seen at the limb has been shown to indicate near-term eruption (Forland et al., 2013). Once the eruption occurs, these views improve forecasts of CME geo-effectiveness. The so-called "stealth" CMEs (Robbrecht et al., 2009) have no obvious coronal sources when viewed from the SEL, but such Earth-directed CMEs would be readily detected from a coronagraph at a polar or quadrature vantage. These extra-SEL viewpoints also more accurately measure CME speed and mass (and hence, kinetic energy). For example, the accuracy of the CME time of arrival at Earth has improved to 6–7 h from 24 h in the pre-STEREO era (Colaninno et al., 2013). There are early indications that the momentum flux of the Earth-directed part of a CME front, measured from a extra-SEL coronagraph, can be extrapolated to 1 AU and used to predict Dst variations (Savani et al., 2013).

Of utmost importance, extra-SEL configurations seem to be our best option for quantifying the magnetic field entrained in the CME. We note that from the poles, the line-of-sight field is B_z, the North-South component known to greatly impact geoeffectiveness. Line-of-sight B_z could potentially be obtained, even mapped, via Faraday rotation measured from beacon signals sent from spacecraft distributed in and away from the ecliptic (e.g., Jensen et al., 2013). Or, as recent analysis of a simulated CME has demonstrated, coronal IR spectropolarimetry has the potential to observe line-of-sight magnetic field strength at the core of an erupting CME (**Figure 6**, Fan, in press).

In addition to improved forecast capability, extra-SEL measurements are the best means for monitoring evolution of Earth-intersecting CMEs (and CIRs) via heliospheric imaging, as discussed in section 3.3. The STEREO HIs demonstrated that it is possible to spatially resolve and track CMEs to 1 AU (Davis et al., 2009; DeForest et al., 2013), but they did so at the expense of long exposure and low spatial resolution. Future measurements with improved sensitivity and polarization capability could resolve the inner structure of CMEs, measure the

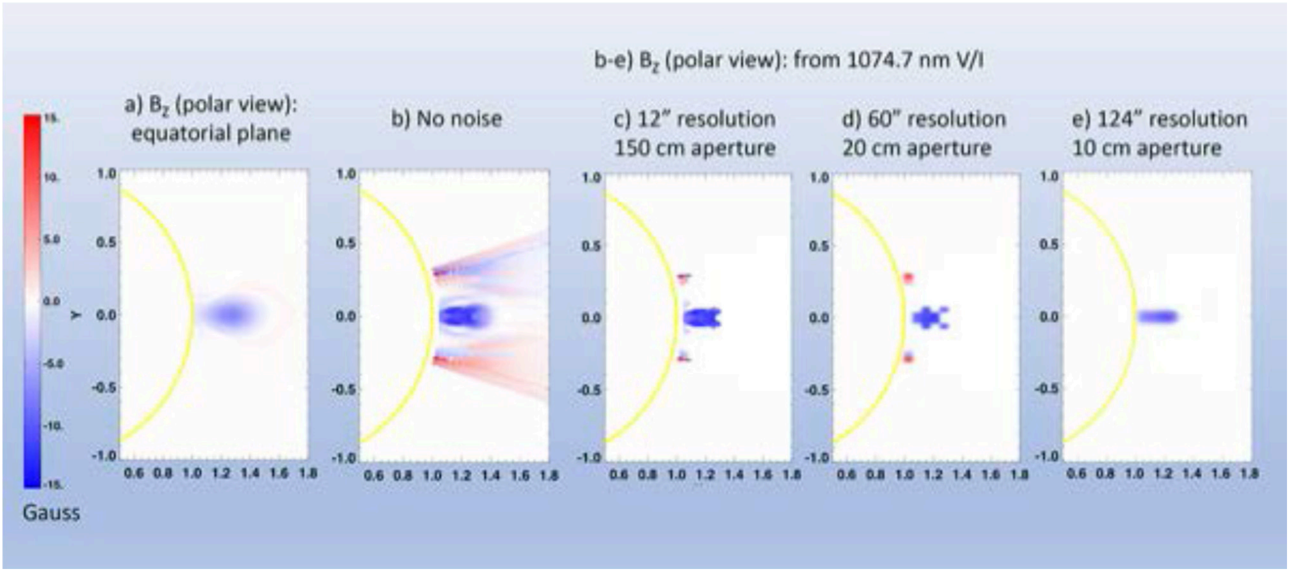

FIGURE 6 | The North-South component of a simulated, erupting CME (Fan, in press) as viewed from the solar North pole. **(A)** Simulation ground truth B_Z in equatorial plane. **(B)** B_Z inverted from ratio of forward-modeled (Gibson et al., 2016) Stokes circular polarization V and intensity I. **(C)** B_Z values with signal-to-noise ratio > 3, based on a 1.5 m telescope, 12″ spatial resolution, and 5 min integration. This is essentially the same as Fan (in press) Figure 12c, except without the background scatter included in that paper appropriate to ground-based telescopes. **(D)** Same except for 20 cm telescope and 60″ resolution. **(E)** Same except for 10 cm telescope and 124″ resolution. Note that the sign and strength of the pre-eruptive core field is captured for all.

standoff distance between CMEs and their shocks, investigate in detail the interaction between CMEs and establish whether CMEs distort, rotate, and/or change propagation direction.

For many of these measurements, the optimal viewpoint lies outside the ecliptic plane (see **Table 4**). Imaging of the inner heliosphere from a polar-viewing spacecraft along the solar rotation axis should provide direct evidence of the Parker spiral structure of the heliosphere, allow the precise mapping of CIRs and CMEs relative to them, and enable study of the angular momentum coupling between the Sun and CMEs. Moreover, as **Figure 5** shows, full 360° longitudinal coverage from a polar-viewing spacecraft provides space-weather monitoring for all the planets and spacecraft in the inner heliosphere, not just the Earth-Moon system and L1. This benefit will become more and more important as human exploration expands out into the heliosphere. In particular, future human exploration to Mars and beyond will require heliosphere-wide space weather monitoring, forecasting, and early-warning outside of the SEL. A polar viewing spacecraft would be able to provide this capability.

Finally, as described in section 3.2, extra-SEL line observations of the photospheric and chromospheric magnetic field improves the boundary condition used in models of both localized source regions and the global solar wind through which transients propagate. Multi-viewpoint measurements of coronal properties can be used to further constrain and drive operational models, which can then be validated with *in-situ* measurements at the Earth. Paired with extra-SEL coronagraph/heliospheric imaging and tracking of the CME core, extra-SEL magnetic observations and data-constrained models could lead to a comprehensive system for forecasting CME impact (e.g., Savani et al., 2015, 2017). The quadrature vantage provides improved irradiance measurements enabling better modeling of the thermosphere/ionosphere. The polar vantage provides benefits to both Earth and planetary space-weather prediction and monitoring.

5. DISCOVERY SPACE

Opportunities for discoveries by extra-SEL spacecraft abound. In addition to the broad range of discoveries likely to arise in association with the science topics described in the previous sections, previous experience shows that unique perspectives may be gained on celestial objects such as comets and asteroids: Ulysses, for example, crossed through the tail of one of the comets that was imaged–and detected *in-situ*–by STEREO (Fulle et al., 2007; Neugebauer et al., 2007). Extra-SEL viewpoints also can extend the observations of variable stars and improve the rate of discovery of exoplanets (Wraight et al., 2011).

The polar view in particular offers unprecedented opportunities for discovery. Stellar activity cycles are monitored and related to the Sun's activity cycle through measurements, for example the Ca K line integrated over the solar disk as viewed from the Sun-Earth line (Wilson, 1978; Baliunas et al., 1995; Egeland et al., 2017). How might these solar measurements change if obtained from the poles? What are the implications for solar twins, which may be observed from a variety of angles relative to their rotation axes? In general, observing from the poles could enable an unprecedented characterization of solar spectral irradiance, with as-yet-to-be-determined impact on our understanding of the Sun as a star, as well as on our

TABLE 4 | Space-weather prediction and modeling enabled by extra-SEL observations.

Open science questions	How can we improve prediction of space weather on time scales of days, weeks, months, or longer? How can we improve forecasts of space-weather impacts at the Earth and throughout the solar system?			
Measurements needed	(1) Full-disk Doppler vector magnetographs (photosphere) (2) Chromospheric spectropolarimeters (3) Full-Sun multiwavelength coronal imagers (4) Multiwavelength coronal spectrometers (5) Polarimetric coronagraphs (6) White-light/multiwavelength coronagraphs (7) Heliographic imagers (HIs) with polarizers (8) *In-situ* solar wind measurements (9) Faraday rotation (e.g., beacon signals between spacecraft and Earth) (10) Irradiance monitors			
Benefits from extra-SEL vantage (assumes existence of complementary SEL observations)		**Polar**	**Quadrature**	**Far-side**
	Longitudinal coverage enabling monitoring of developing coronal holes, active longitudes, etc. that drive "seasons" of space weather	Yes (1; 3; 6)	Yes (1; 3; 6)	Yes (1; 3; 6)
	Improved modeling and monitoring of Earth-intersecting transients	Yes (1–9)	Yes (1–9)	No
	Improved modeling and monitoring of planet-intersecting transients	Yes (1–9)	Sometimes (1–9)	Sometimes (1–9)
	Line-of-sight measurements of southward-directed magnetic field	Yes (5; 9)	No	No
	Improved irradiance measurements	No	Yes (3; 10)	No

understanding of stellar activity in general (Shapiro et al., 2014, 2016).

Beyond this–we have never observed the solar poles with imagers. What will we see? The semi-annual view of high latitudes arising from the tilt of the Earth's orbit provides us with some sense of what we might expect in polar flow patterns, as does SEL observations of high-latitude large-scale magnetic features structures (**Figures 7A,B**). However, based on recent images from planetary missions, such as Juno and Cassini (**Figures 7C,D**), direct observations of the poles is likely to reveal far more complex and beautiful structure than anything we have been able to piece together to date.

6. FUTURE MISSIONS AND GAP ANALYSIS

We have shown that extra-SEL observations have potential for transformative progress in a range of science areas. **Tables 1–4** describe the measurements needed from the various extra-SEL vantages that would lead to such progress. We now discuss plans for future missions, and consider how the gaps in our current observational capability may be filled.

6.1. Near-Term Extra-SEL Missions: Solar Orbiter and Parker Solar Probe

The upcoming Parker Solar Probe (PSP), scheduled for launch in August of 2018, will explore the outer corona and inner heliosphere with very rapid solar encounters, starting at a perihelion of $35.7R_{\odot}$ in November 2018 (already twice as close to the Sun as Helios ever went) and reaching its minimum perihelion of $9.86R_{\odot}$ in late 2024 (Fox et al., 2016). In addition, the Solar Orbiter (SO) mission, to be launched no earlier than February 2020, will orbit the sun between 0.28 and $0.7AU$ and reach a maximum inclination of $\approx$ 30–34° out of the ecliptic by the end of its extended mission in 2029–2030 (Müller et al., 2013). **Figure 8** shows sample orbits for both spacecraft.

Thanks to its gradually diminishing perihelion, PSP will directly probe the state of the solar wind as it evolves from its magnetically-dominated regime in the corona to the flow-dominated regime we experience at 1 AU. The critical heights where this occurs are collectively referred to as the "Alfvén surface," although density inhomogeneity may be so great as to disrupt any real smooth surface (DeForest et al., 2018). Theoretical models place the critical heights between 12 and $30R_{\odot}$, depending on the location and phase of the solar cycle (Verdini et al., 2009; Katsikas et al., 2010; Zhao and Hoeksema, 2010; Goelzer et al., 2014; Tasnim and Cairns, 2016). These heights will become accessible to PSP within 2 years from launch and enable long-desired studies of the level of turbulence, heating, and kinematics of the primary constituents of the solar wind (i.e., electrons, protons, and helium). These, in turn, will unveil the energy flow from the sun to the heliosphere and help us pinpoint the mechanism responsible for solar wind heating and acceleration. PSP will spend 400 h below $15R_{\odot}$ (75 h below $12R_{\odot}$) over 5 years and thus measure the trans-Alfvénic solar wind properties during a considerable part of the solar cycle and over a multitude of locations and activity levels. The radial and longitudinal scans, enabled by the close perihelia, will help to uncover the role of reconnection jets and instabilities in the heating and acceleration of the solar wind.

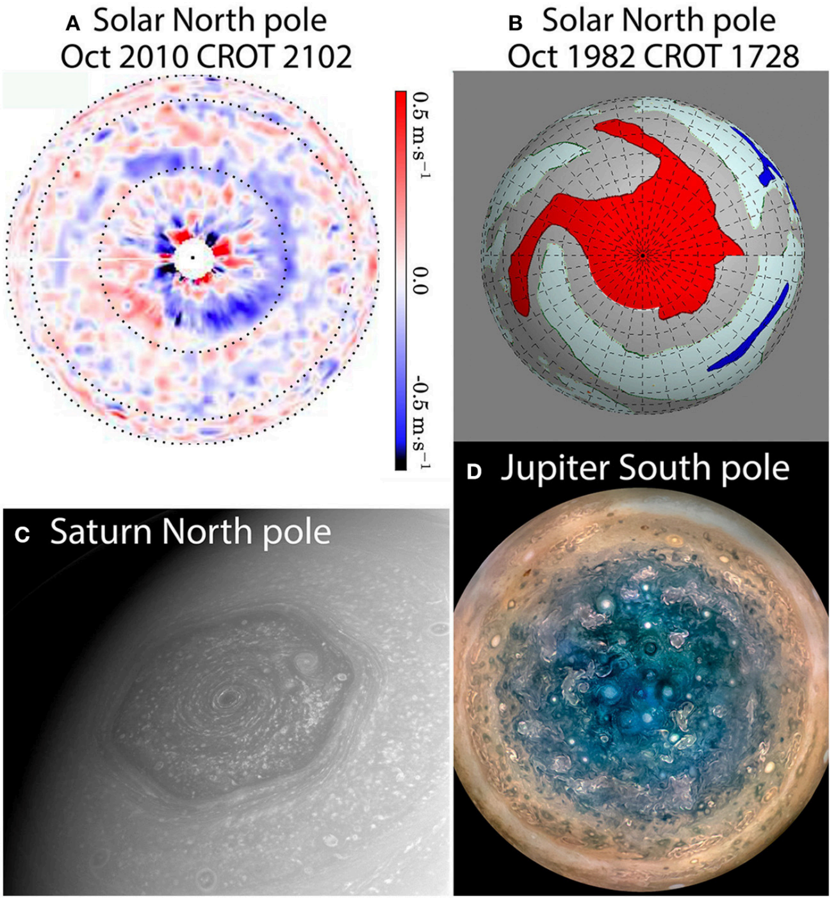

FIGURE 7 | (A) Ring-diagram analysis of near-surface flow anomalies indicate spiral flow patterns at the poles (from Bogart et al., 2015; Copyright ©AAS. Reproduced with permission). **(B)** Observations of large-scale, high-latitude magnetic features spanning multiple decades (McIntosh et al., 1976; McIntosh, 2003) similarly demonstrate spiral structure at the poles (from Webb et al., 2018) (red = negative coronal hole, blue = positive coronal hole, gray = negative polarity quiet Sun, light blue = positive polarity quiet Sun, dark green = filaments). **(C)** A view centered on Saturn's north pole. North is up and rotated 33° to the left. The image was taken with the Cassini spacecraft wide-angle camera on June 14, 2013 using a spectral filter sensitive to wavelengths of near-infrared light centered at 752 nm (Source: NASA JPL). **(D)** Multiple images combined show Jupiter's south pole, as seen by NASA's Juno spacecraft from an altitude of 32,000 miles. The oval features are cyclones. (Credit: NASA/JPL - Caltech/SwRI/MSSS/Betsy Asher Hall/Gervasio Robles).

In addition, PSP will provide the first measurements of the energetic particle populations in the solar corona and allow the separation of transport vs. production effects in energetic particles. This has been a stumbling block in deciphering the mechanisms responsible for particle acceleration in astrophysical plasmas for decades.

In close synergy, SO will obtain similar, but outside-the-ecliptic, *in-situ* measurements that will help to unravel the latitudinal structure and flow of energy (and energetic particles) in the inner heliosphere. Combined with the first ever direct measurements of the polar magnetic fields, the SO mission will considerably narrow uncertainty for global solar and heliospheric plasma and magnetic field modeling, leading to breakthroughs in many research areas, including solar dynamo evolution, energetic particle transport, and space-weather forecasting. Unlike PSP, SO has a full complement of solar and coronal imaging instruments capable of very high spatial resolution measurements ($< 300km$) during perihelia to help uncover the physical processes behind eruptive events (i.e., magnetic reconnection) that are thought to occur at small spatial scales. SO instruments also span a broad spectral range, and include an X-ray spectrometer that in conjunction with SEL observations will enable spectroscopic analysis of solar flares at high energy, helping to distinguish between flare acceleration models (Casadei et al., 2017). Finally, SO's strongest contributions will likely be to deciphering the connectivity between solar and heliospheric magnetic structures and plasmas, thanks to its unique combination of remote sensing and *in-situ* instruments.

Although we expect PSP and SO to lead to groundbreaking advances in several of the open science questions discussed above, the two missions will not fully address the open questions listed above for several reasons. PSP and SO are designed to meet specific science objectives—pertaining to the acceleration, heating, and structure of the solar wind—via *encounter mission*

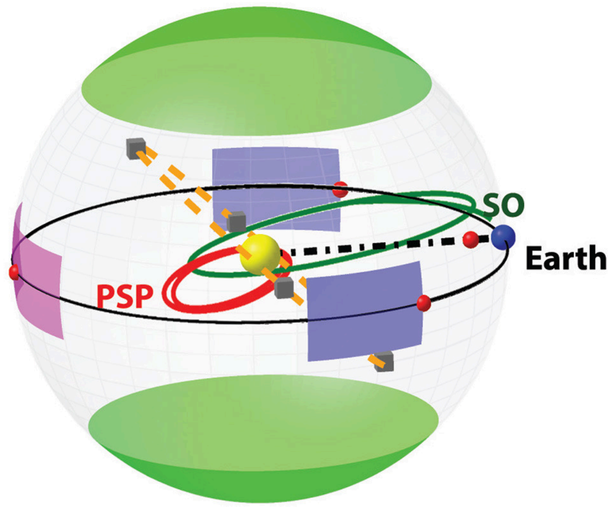

FIGURE 8 | Interesting viewpoints shown as in **Figure 1**, with Parker Solar Probe (PSP; red) and Solar Orbiter (SO; green) orbits overlaid. The dashed orange line represents a sample "diamond" orbit with four spacecraft (gray cubes) 90° apart, reaching as high as 75° heliolatitude (Vourlidas, 2017). The colored patches on the 1AU sphere are the same as in **Figure 1**.

designs. This means that the instruments operate for limited amounts of time per orbit (10 days for PSP, 30 days for the SO remote sensing payload). Other complications include restricted data volumes due to the limited number of downlinks and onboard storage, data latency on the order of months, and angular configurations between the two spacecraft and Earth that are continuously changing.

These operational constraints reduce the length of polar magnetic field observations by SO, for example, to only a few days per orbit (up to 10 days per orbit by the end of the extended mission). The shortness of this time period will limit helioseismology studies (Löptien et al., 2015). The data volumes and short observing periods also do not allow for synoptic observations or consistent 360° coverage of the solar atmosphere from the SO imagers. PSP imaging is restricted to a wide field heliospheric imager providing context for the *in-situ* payload but has no disk imaging (for thermal reasons).

It is undeniable that both missions will provide unique data and views of the coronal and heliospheric environment, and enhance the sophistication of multi-viewpoint analysis, far beyond STEREO. However, they are necessarily limited to the science achievable by the instruments they have on board, and in their ability to obtain the sustained measurements needed for longer-time-frame studies and space-weather monitoring (see **Table 4**). We now consider how next-generation extra-SEL mission concepts might address the remaining gaps between the observational capabilities of our existing and planned missions, and the outstanding science questions raised in this paper.

6.2. Missions for the Future

Several white papers describing extra-SEL mission concepts were submitted during the last Solar and Space Physics Decadal Survey activies, and were also summarized in the 2014 Heliophysics Roadmap. Variations of those concepts were submitted for the Next Generation Solar Physics Mission call for ideas. The majority of these white papers are not in the published literature, but a subset, with emphasis on helioseismology science, is discussed by Sekii et al. (2015). Here, we present some representative concepts for mission architectures that emphasize sustained measurements, and so fill most, if not all, of the gaps indicated by **Table 5** (depending on instrument payload).

6.2.1. Quadrature Mission

The idea of a mission to the Lagrange L5 point has been explored in several concepts in recent years (Webb et al., 2010; Gopalswamy et al., 2011; Vourlidas, 2015; Lavraud et al., 2016). It has obvious advantages for space-weather research and forecasting, such as more accurate speed measurements for Earth-directed CMEs and increased coverage of solar irradiance and the photospheric magnetic boundary for operational models. It also addresses many of the open science questions that particularly benefit from sustained measurements, such as probing the solar interior more deeply, and observing the evolution of structures over time, as well as 3D modeling of CMEs and their source regions. Such analyses depend upon the existence of complementary SEL observations.

From the mission design perspective, injection toward the L5 (and L4) points is relatively straightforward but requires significant ΔV and hence a large rocket. There is considerable trade space: orbit around L5 vs. stationed at L5, drift vs. direct injection, and travel time vs. mission length, to name a few. Indeed, it is also possible to put something at 90–120° off the SEL utilizing a launch into a geo-transfer orbit and electric propulsion.

An L5 concept was studied for the Solar and Space Physics Decadal Survey, and estimated to cost above $600M(FY14)$ for a standard spacecraft with multiple instruments. An operational space-weather mission to L5 could be cheaper if it had a reduced payload—at minimum, a coronagraph and a magnetograph–as was the case studied by Trichas et al. (2015). As of the writing of this paper, the European Space Agency (ESA) is in Phase-A development for an operational L5 mission.

An innovative approach based on a fractionated spacecraft concept was also proposed by Liewer et al. (2009). Instead of a monolithic spacecraft carrying a multitude of instruments, the authors proposed the launch of a set of cubesats or minisats each carrying a single telescope along with a minisat carrying a standard antenna to relay communications from the constellation to Earth. The advantages include (1) lower launch costs through extensive use of hosted payload opportunities, (2) measurement persistence, since failed cubesats or telescopes could be replaced with another launch, and (3) redundancy, since a single spacecraft failure would not take down the whole constellation. The disadvantages include (1) the necessarily reduced size of instrument payloads, leading to restrictions on aperture size and other performance metrics, (2) data acquisition limitations—since cubesats have less powerful radios and smaller antennas, and (3) the low Technology Readiness Levels (TRLs) for intra-spacecraft communications and of interplanetary cubesats.

TABLE 5 | Gap analysis.

Measurements needed	Vantages
(1) Full-disk Doppler vector magnetographs (photosphere)	Polar (P), Quadrature (Q), Far-side (F)
(2) Chromospheric spectropolarimeters	
(3) Full-Sun multiwavelength coronal imagers	
(4) Multiwavelength coronal spectrometers	
(5) Polarimetric coronagraphs	
(6) White-light/multiwavelength coronagraphs	
(7) Heliographic imagers (HIs) with polarizers (note: 7′ below indicates HIs that do not have polarizers)	
(8) *In-situ* solar wind measurements	
(9) Faraday rotation (e.g., beacon signals between spacecraft and Earth)	
(10) Irradiance monitors	

Benefits from extra-SEL vantage (assumes existence of complementary SEL observations)	**Measurements and vantages** (see above)	**STEREO**	**SO**	**PSP**
Helioseismic inversions probe deeper	1 P/Q/F	No	Limited	No
Better coverage of global magnetic boundary; Comprehensive view of flux emergence and evolution	1 P/Q/F	No	Limited	No
Polar fields and flows directly observed; Magnetic vector boundary disambiguated	1–2 P; 1–2 P/Q	No	Yes (1)	No
Input to coronal 3D modeling	3–6 P/Q	Yes (3; 6)	Yes (3; 4; 6)	No
More lines of sight to reconstruct 3D solar wind structures	6–7 P/Q	Yes (6-7′)	Yes (6–7′)	Limited (7′)
Simultaneous boundary/limb views of CMEs and precursors; global interactions comprehensively observed	1–6 P/Q	Yes (3; 6)	Limited (1; 3; 4; 6)	No
Solar-wind source regions connected to heliospheric imaging and *in-situ* measurements	1–8 P/Q	Yes (3; 6; 7′)	Yes (1; 3; 4; 6; 7′; 8)	Yes (7′; 8)
Longitudinal structure of the Alfvén surface and of CMEs, CIRs, and shocks revealed	6; 7 P	No	No	No
Improved monitoring and modeling of Earth-intersecting (planet-intersecting) transients.	1–9 P/Q (P/Q/F)	Limited (3; 6; 7′)	Limited (1; 3; 4; 6; 7′; 8)	Limited (7′; 8)
Longitudinal coverage enabling monitoring “seasons” of space weather	1; 3; 6 P/Q/F	Limited (3)	Limited (1; 3; 6)	No
Improved irradiance measurements enabling better measurements of the thermosphere/ionosphere	3; 10 Q	Limited (3)	No	No
Line-of-sight measurement of southward-directed magnetic field	5; 9 P	No	No	No

In summary, a mission to L5 or similar quadrature viewpoint seems to be the obvious next step after STEREO. The benefits of this vantage for an operational space-weather mission are particularly strong. The benefits for basic research are also high; however, as we will now discuss, a polar vantage achieves these same benefits, and more.

6.2.2. Solar Polar Imager (Single and Constellation)

Imaging of the solar poles has been a long-held desire of the solar community ever since the cancellation of the imaging sister payload to Ulysses. Mission concepts have been proposed for the ESA large mission competition (e.g., POLARIS Appourchaux et al., 2009, 2014), and the Chinese space program (SPORT Xiong and Liu, 2014). The primary scientific objective of these missions is the unique opportunities they provide for measuring the evolving polar magnetic field and for investigating sub-surface flows beneath the poles via helioseismology. As **Table 5** demonstrates, further unique science is achieved from a polar vantage pertaining to the longitudinal structure of the coronal streamer belt, Alfvén surface, and transient/solar wind interactions. Moreover, the space-weather and basic-research open questions pertaining to 3D modeling of CMEs and their source regions and solar wind interactions are also achieved from a polar vantage. Finally, the polar vantage provides the most opportunities for discovery as discussed in section 5.

Achieving high inclinations has traditionally been the stumbling block for the realization of such polar missions. A Jupiter gravity assist, as was done for the Ulysses mission, remains the most practical method for going over the poles. However, this approach also implies that aphelion occurs near Jupiter, resulting in a very long orbit with only a small fraction of time spent close to the Sun. The SPORT approach adds Venus-Jupiter gravity assists to reduce the perihelion to about 0.7 AU and shorten the orbit somewhat. However, time above the poles (defined here as above 60°) remains a small portion of the overall orbit. The window of science operations can be extended for orbits within 0.8 AU but the Venus gravity alone limits the inclination maximum to about 34°, with chemical propulsion. For this reason, many solar-polar mission concepts use solar sails (150 × 150 m) to achieve high inclinations, presenting challenges associated with the large size and low TRL of solar-sail technology.

Given the high scientific value and significant opportunity for discovery of a solar polar imaging mission, new mission concepts continue to be developed (Hassler et al., 2018a,b). In particular, advances in new spacecraft technology and instrument miniaturization are enabling new mission concepts to achieve the core science objectives of a polar imaging mission. For example, a new version of a solar polar mission [Solar Polar Explorer (SOLPEX)] has been developed (Newmark, 2018) using a combination of a Jupiter gravity assist and solar electric propulsion [e.g., NASA Evolutionary Xenon Thruster (NEXT) thrusters] to achieve a high inclination ($> 75^\circ$) orbit with an eventual $\approx$ 1 year period (final orbit is 0.5×1.5 AU). SOLPEX would contain a suite of remote sensing (Doppler magnetograph, EUV imager, coronagraph, and heliospheric imager) and *in-situ* instruments, and could complete three passes over each of the solar poles within a 9 year mission lifetime, with each pass lasting $>$ 38 days above 60°.

A wide range of instrumentation could reveal new information from a polar view (**Table 5**). The fractionated approach might lend itself well to a polar strategy, with minisats carrying smaller instruments (e.g., magnetograph, EUV imager, and/or compact coronagraph) that would provide continuous 360° coverage. Larger missions could carry other, more state-of-the-art instrumentation to fill in the other science gaps that we have identified. Such an approach would allow the participation of multiple international space agencies, so that over time, a truly global perspective on the Sun and heliosphere would be achieved.

A final consideration: a single spacecraft in polar orbit would still spend a finite time over the poles. Truly sustained polar observations could be achieved by the deployment of a constellation of spacecraft. For example, four spacecraft spaced 90° apart in diamond formation (**Figure 8** and Vourlidas, 2017) would provide continuous, complete 360° coverage of the solar atmosphere, from the photosphere to the corona and beyond (depending on the payload). Such a concept would also reduce the need for coverage in the ecliptic plane.

7. CONCLUSIONS

Extra-SEL vantages present unique opportunities for answering the outstanding science questions of heliophysics, for improving space-weather monitoring and prediction, and for revealing new discoveries about our Sun and solar system. A broad range of observations take on new significance away from the SEL, including both remote-sensing and *in-situ* measurements.

We have discussed the benefits of measurements from several types of instrumentation in this paper (**Table 5**), but have not attempted to put these in priority order. A promising path forward in establishing the relative importance of different measurements is to combine comprehensive models of the solar physical state with forward modeling of observables (see e.g., Gibson, 2015). In particular, sensitivity analyses that evaluate how different types of observations at different vantages constrain and improve model-data fitting are essential for establishing the most-urgently needed new measurements (see e.g., Kramar et al., 2006; Mackay et al., 2016; Pevtsov et al., 2016).

All three of the vantages considered in this paper–polar, quadrature, and far-side–are of interest. It should be noted, however, that **Tables 1–5** considered these vantages independently, while a mission such as STEREO obtains both quadrature and and far-side vantages, and similarly, a mission in a high-latitude orbit may view the far side or quadrature as it crosses the ecliptic. Moreover, in **Tables 1–5** we assumed only the availability of complementary SEL observations; clearly, if both quadrature and far-side measurements were available, many of the two-view benefits ascribed only to the quadrature-SEL or polar-SEL combinations would be realized.

Bearing this in mind, it is nevertheless a worthwhile exercise to consider the science enabled by the three vantages independently as we have done, and in particular to focus on the benefits of *sustained* observations from these vantages. The far-side and quadrature vantages have the advantage of being relatively easy to access, and the use of a Doppler magnetograph from both would enable global magnetic coverage and deeper helioseismic inversions. The quadrature vantage would also provide a second line of sight on structures visible along the SEL, enabling 3D reconstructions. A sustained view would allow constant monitoring of transients directed along the SEL, providing substantial space-weather operational benefit. The polar vantage is the most compelling overall, as it would achieve essentially the same capabilities as from quadrature, and also reveal the poorly observed poles as never before. For this reason, it is essential that investment in and demonstration of the technologies needed for polar missions are prioritized over the next few years. In this way, the groundwork may be laid so that by the next decadal survey, community proposals for solar polar missions will not only be scientifically justified, but technologically robust.

AUTHOR CONTRIBUTIONS

MT, SG, LR, MV, AT, and SM contributed to the initial conception and design of the paper. SG wrote the main draft and coordinated inputs. AV, DH, LR, MT, MV, and JN contributed text and figures. All of the authors read and critically revised the paper, approved the final version, and agreed to be accountable for all aspects of the work.

FUNDING

NCAR is supported by the National Science Foundation. AV is supported by NNX16AH70G under the STEREO MO&DA and NRL grant N00173-16-1-G029.

ACKNOWLEDGMENTS

We thank Yuhong Fan for providing the simulation data cube used in **Figure 6**, and Mark Miesch for many helpful discussions. We also thank Ricky Egeland for internal HAO review of the manuscript.

REFERENCES

Appourchaux, T., Auchère, F., and Antonucci, E. E. (2014). "SOLARIS: Solar Sail Investigation of the Sun" in *Advances in Solar Sailing, Vol. 259*, ed M. Macdonald (Berlin; Heidelberg: Springer), 259–268.

Appourchaux, T., Liewer, P., Watt, M., Alexander, D., Andretta, V., Auchère, F., et al. (2009). POLAR investigation of the Sun - POLARIS. *Exp. Astron.* 23, 1079–1117. doi: 10.1007/s10686-008-9107-8

Arge, C. N., Harvey, K. L., Hudson, H. S., and Kahler, S. W. (2003). "Narrow coronal holes in Yohkoh soft X-ray images and the slow solar wind," in *Solar Wind Ten, Vol. 679*, American Institute of Physics Conference Series, eds M. Velli, R. Bruno, F. Malara, and B. Bucci (College Park, MD: AIP Publishing), 202–205.

Arge, C. N., Henney, C. J., Koller, J., Compeau, C. R., Young, S., MacKenzie, D., et al. (2010). "Air force data assimilative photospheric flux transport (ADAPT) model," in *Twelfth International Solar Wind Conference* (College Park MD: AIP Publishing), 343–346.

Aschwanden, M. J. (2011). Solar stereoscopy and tomography. *Living Rev. Solar Phys.* 8:5. doi: 10.12942/lrsp-2011-5

Aschwanden, M. J., Schrijver, C. J., and Malanushenko, A. (2015). Blind stereoscopy of the coronal magnetic field. *Solar Phys.* 290, 2765–2789. doi: 10.1007/s11207-015-0791-z

Bai, T. (1987). Distribution of flares on the sun - Superactive regions and active zones of 1980-1985. *Astrophys. J.* 314, 795–807. doi: 10.1086/165105

Baliunas, S. L., Donahue, R. A., Soon, W. H., Horne, J. H., Frazer, J., Woodard-Eklund, L., et al. (1995), Chromospheric variations in main-sequence stars. *Astrophys. J.*. 438, 269–287. doi: 10.1086/175072

Balogh, A., Beek, T. J., Forsyth, R. J., Hedgecock, P. C., Marquedant, R. J., Smith, E. J., et al. (1992). The magnetic field investigation on the Ulysses mission instrumentation and preliminary scientific results. *A&AS* 92:221.

Bame, S., McComas, D., Barraclough, B., Phillips, J., Sofaly, K., Chavez, J., et al. (1992). The Ulysses solar-wind plasma experiment. *Astron. Astrophys. Supp. Series* 92, 237–265.

Basu, S., and Antia, H. M. (2008). Helioseismology and solar abundances. *Phys. Rep.* 457, 217–283. doi: 10.1016/j.physrep.2007.12.002

Bird, M. K., Volland, H., Howard, R. A., Koomen, M. J., Michels, D. J., Sheeley, N. R. Jr., et al. (1985). White-light and radio sounding observations of coronal transients. *Solar Phys.* 98, 341–368. doi: 10.1007/BF00152465

Bogart, R. S., Baldner, C. S., and Basu, S. (2015). Evolution of near-surface flows inferred from high-resolution ring-diagram analysis. *Astrophys. J.* 807:125. doi: 10.1088/0004-637X/807/2/125

Bosman, E., Bothmer, V., Nisticò, G., Vourlidas, A., Howard, R. A., and Davies, J. A. (2012). Three-dimensional properties of coronal mass ejections from STEREO/SECCHI observations. *Solar Phys.* 281, 167–185. doi: 10.1007/s11207-012-0123-5

Casadei, D., Jeffrey, N. L. S., and Kontar, E. P. (2017). Measuring X-ray anisotropy in solar flares. Prospective stereoscopic capabilities of STIX and MiSolFA. *aap*. 606:A2. doi: 10.1051/0004-6361/2017 30629

Castenmiller, M. J. M., Zwaan, C., and van der Zalm, E. B. J. (1986). Sunspot nests - Manifestations of sequences in magnetic activity. *Solar Phys.* 105, 237–255. doi: 10.1007/BF00172045

Chang, H.-K., Chou, D.-Y., Labonte, B., and TON Team (1997). Ambient acoustic imaging in helioseismology. *Nature* 389, 825–827. doi: 10.1038/39822

Charbonneau, P. (2010). Dynamo models of the solar cycle. *Living Rev. Solar Phys.* 7:3. doi: 10.12942/lrsp-2010-3

Christensen-Dalsgaard, J. (2002). Helioseismology. *Rev. Mod. Phys.* 74, 1073–1129. doi: 10.1103/RevModPhys.74.1073

Christensen-Dalsgaard, J., and Thompson, M. J. (2007). "Observational results and issues concerning the tachocline," in *The Solar Tachocline,* eds D. W. Hughes, R. Rosner, and N. O. Weiss (Cambridge, UK: Cambridge University Press), 53.

Colaninno, R. C., Vourlidas, A., and Wu, C. C. (2013). Quantitative comparison of methods for predicting the arrival of coronal mass ejections at Earth based on multiview imaging. *J. Geophys. Res.* 118, 6866–6879. doi: 10.1002/2013JA019205

Colin, L. (1980). The Pioneer Venus program. *J. Geophys. Res.* 85, 7575–7598. doi: 10.1029/JA085iA13p07575

Davis, C. J., Davies, J. A., Lockwood, M., Rouillard, A. P., Eyles, C. J., and Harrison, R. A. (2009). Stereoscopic imaging of an Earth-impacting solar coronal mass ejection: a major milestone for the STEREO mission. *Geophys. Res. Lett.* 36:L08102. doi: 10.1029/2009GL038021

De Rosa, M. L., Schrijver, C. J., Barnes, G., Leka, K. D., Lites, B. W., Aschwanden, M. J., et al. (2009). A critical assessment of nonlinear force-free field modeling of the solar corona for active region 10953. *Astrophys. J.* 696, 1780–1791. doi: 10.1088/0004-637X/696/2/1780

de Toma, G., White, O. R., and Harvey, K. L. (2000). A picture of solar minimum and the onset of solar cycle 23. I. Global magnetic field evolution. *Astrophys. J.* 529, 1101–1114. doi: 10.1086/308299

DeForest, C., Howard, R. A., Velli, M., Viall, N., and Vourlidas, A. (2018). The highly-structured outer solar corona. *Astrophys. J.* 862:18. doi: 10.3847/1538-4357/aac8e3

Deforest, C. E., Hoeksema, J. T., Gurman, J. B., Thompson, B. J., Plunkett, S. P., Howard, R., et al. (1997). Polar plume anatomy: results of a coordinated observation. *Solar Phys.* 175, 393–410. doi: 10.1023/A:1004955223306

DeForest, C. E., Howard, T. A., and McComas, D. J. (2013). Tracking coronal features from the low corona to Earth: a quantitative analysis of the 2008 December 12 Coronal Mass Ejection. *Astrophys. J.* 769:43. doi: 10.1088/0004-637X/769/1/43

DeForest, C. E., Howard, T. A., and McComas, D. J. (2014). Inbound waves in the solar corona: a direct indicator of Alfven surface location. *Astrophys. J.* 787:124. doi: 10.1088/0004-637X/787/2/124

DeForest, C. E., Howard, T. A., Webb, D. F., and Davies, J. A. (2016). The utility of polarized heliospheric imaging for space weather monitoring. *Space Weather* 14, 32–49. doi: 10.1002/2015SW001286

Duvall, T. L., Jr, Jefferies, S. M., Harvey, J. W., and Pomerantz, M. A. (1993). Time-distance helioseismology. *Nature* 362, 430–432. doi: 10.1038/362430a0

Egeland, R., Soon, W., Baliunas, S., Hall, J. C., Pevtsov, A. A., and Bertello, L. (2017). *VizieR Online Data Catalog: Calibrated Solar S-Index Time Series (Egeland+, 2017)*. VizieR Online Data Catalog, 183.

Elsworth, Y., Howe, R., Isaak, G. R., McLeod, C. P., Miller, B. A., New, R., et al. (1994). Solar p-mode frequencies and their dependence on solar activity recent results from the BISON network. *Astrophys. J.* 434, 801–806. doi: 10.1086/174783

Fan, Y. (in press). MHD simulation of a prominence eruption. *Astrophys. J.* doi: 10.3847/1538-4357/aaccee

Forland, B. F., Gibson, S. E., Dove, J. B., Rachmeler, L. A., and Fan, Y. (2013). Coronal cavity survey: morphological clues to eruptive magnetic topologies. *Solar Phys.* 288, 603–615. doi: 10.1007/s11207-013-0361-1

Fox, N. J., Velli, M. C., Bale, S. D., Decker, R., Driesman, A., Howard, R. A., et al. (2016). The Solar Probe Plus mission: humanity's first visit to our star. *Space Sci. Rev.* 204, 7–48. doi: 10.1007/s11214-015-0211-6

Fulle, M., Leblanc, F., Harrison, R. A., Davis, C. J., Eyles, C. J., Halain, J. P., et al. (2007). Discovery of the atomic iron tail of comet McNaught using the heliospheric imager on STEREO. *Astrophys. J. Lett.* 661, L93–L96. doi: 10.1086/518719

Gabriel, A. H., Charra, J., Grec, G., Robillot, J.-M., Roca Cortés, T., Turck-Chièze, S., et al. (1997). Performance and early results from the GOLF instrument flown on the SOHO mission. *Solar Phys.* 175, 207–226. doi: 10.1023/A:1004911408285

Gibson, S. (2015). "Data-model comparison using FORWARD and CoMP," in *IAU Symposium, Vol. 305* (Cambridge, UK: Cambridge University Press), 245–250.

Gibson, S., Kucera, T., White, S., Dove, J., Fan, Y., Forland, B., et al. (2016). FORWARD: a toolset for multiwavelength coronal magnetometry. *Front. Astron. Space Sci.* 3:8. doi: 10.3389/fspas.2016.00008

Gibson, S. E., Kozyra, J. U., de Toma, G., Emery, B. A., Onsager, T., and Thompson, B. J. (2009). If the sun is so quiet, why is the earth still ringing? A comparison of two solar minimum intervals. *J. Geophys. Res.* 114:A09105. doi: 10.1029/2009JA014342

Gizon, L., Birch, A. C., and Spruit, H. C. (2010). Local helioseismology: three-dimensional imaging of the solar interior. *Ann. Rev. Astron. Astrophys.* 48, 289–338. doi: 10.1146/annurev-astro-082708-101722

Gloeckler, G., Geiss, J., Balsiger, H., Bedini, P., Cain, J. C., Fisher, J., et al. (1999). The solar wind ion composition spectrometer. *Astron. Astrophys. Supp. Ser.* 92, 267–289.

Goelzer, M. L., Schwadron, N. A., and Smith, C. W. (2014). An analysis of Alfvén radius based on sunspot number from 1749 to today. *J. Geophys. Res.* 119, 115–120. doi: 10.1002/2013JA019420

Gopalswamy, N., Davila, J. M., St. Cyr, O. C., Sittler, E. C., Auchère, F., Duvall, T. L., et al. (2011). Earth-affecting Solar Causes Observatory (EASCO): a potential International Living with a Star Mission from Sun-Earth L5. *J. Atmos. Solar Terrestr. Phys.* 73, 658–663. doi: 10.1016/j.jastp.2011.01.013

Gurnett, D. A., Anderson, R. R., and Odem, D. L. (1975). The University of Iowa Helios solar wind plasma wave experiment. *Raumfahrtforschung* 19, 245–247.

Hanasoge, S., Miesch, M. S., Roth, M., Schou, J., Schüssler, M., and Thompson, M. J. (2015). Solar dynamics, rotation, convection and overshoot. *Space Sci. Rev.* 196, 79–99. doi: 10.1007/s11214-015-0144-0

Harvey, J. W., Hill, F., Hubbard, R. P., Kennedy, J. R., Leibacher, J. W., Pintar, J. A., et al. (1996). The global oscillation network group (GONG) project. *Science* 272, 1284–1286. doi: 10.1126/science.272.5266.1284

Hassler, D., Newmark, J., Velli, M., and Murphy, N. (2018a). *Proceedings of Solar Wind 15 Conference* (Brussels), 18–22.

Hassler, D., Velli, M., Murphy, N., and Newmark, J. (2018b). AGU meeting. *TESS Conference (21–24 May 2018)*.

Hassler, D. M., Dammasch, I. E., Lemaire, P., Brekke, P., Curdt, W., Mason, H. E., et al. (1999). Solar wind outflow and the chromospheric magnetic network. *Science* 283:810. doi: 10.1126/science.283.5403.810

Hassler, D. M., Wilhelm, K., Lemaire, P., and Schühle, U. (1997). Observations of polar plumes with the SUMER instrument on SOHO. *Solar Phys.* 175, 375–391. doi: 10.1023/A:1004959324214

Hathaway, D. H. (2015). The solar cycle. *Living Rev. Solar Phys.* 12:4. doi: 10.1007/lrsp-2015-4

Hickmann, K. S., Godinez, H. C., Henney, C. J., and Arge, C. N. (2015). Data assimilation in the ADAPT photospheric flux transport model. *Solar Phys.* 290, 1105–1118. doi: 10.1007/s11207-015-0666-3

Hill, F. (1988). Rings and trumpets - Three-dimensional power spectra of solar oscillations. *Astrophys. J.* 333, 996–1013. doi: 10.1086/166807

Hoeksema, J. T., and Scherrer, P. H. (1986). An atlas of photospheric magnetic field observations and computed coronal magnetic fields: 1976-1985. *Solar Phys.* 105, 205–211. doi: 10.1007/BF00156388

Howard, R. A., Moses, J. D., Vourlidas, A., Newmark, J. S., Socker, D. G., P., P. S., et al. (2008). Sun Earth connection coronal and heliospheric investigation (SECCHI). *Space Sci. Rev.* 136:67. doi: 10.1007/s11214-008-9341-4

Howe, R. (2009). Solar interior rotation and its variation. *Living Rev. Solar Phys.* 6:1. doi: 10.12942/lrsp-2009-1

Hurley, K., Sommer, M., Atteia, J.-L., Boer, M., Cline, T., Cotin, F., et al. (1992). The solar X-ray/cosmic gamma-ray burst experiment aboard Ulysses. *Astron. Astrophys.* 92, 401–410.

Isavnin, A., Vourlidas, A., and Kilpua, E. K. J. (2014). Three-dimensional evolution of flux-rope CMEs and its relation to the local orientation of the heliospheric current sheet. *Solar Phys.* 289, 2141–2156. doi: 10.1007/s11207-013-0468-4

Issautier, K., Le Chat, G., Meyer-Vernet, N., Moncuquet, M., Hoang, S., MacDowall, R. J., et al. (2008). Electron properties of high-speed solar wind from polar coronal holes obtained by Ulysses thermal noise spectroscopy: not so dense, not so hot. *Geophys. Res. Lett.* 35:L19101. doi: 10.1029/2008GL034912

Jackson, B. V. (1985). Imaging of coronal mass ejections by the Helios spacecraft. *Solar Phys.* 100, 563–574. doi: 10.1007/BF00158445

Jensen, E. A., Bisi, M. M., Breen, A. R., Heiles, C., Minter, T., and Vilas, F. (2013). Measurements of Faraday rotation through the solar corona during the 2009 solar minimum with the MESSENGER spacecraft. *Solar Phys.* 285, 83–95. doi: 10.1007/s11207-012-0213-4

Kaiser, M. L., Kucera, T. A., Davila, J. M., St. Cyr, O. C., Guhathakurta, M., and Christian, E. (2008). The STEREO mission: an introduction. *Space Sci. Rev.* 136, 5–16. doi: 10.1007/s11214-007-9277-0

Kane, S. R., Hurley, K., McTiernan, J. M., Boer, M., Niel, M., Kosugi, T., et al. (1998). Stereoscopic observations of solar hard X-Ray flares made by Ulysses and YOHKOH. *Astrophys. J.* 500, 1003–1008. doi: 10.1086/305738

Katsikas, V., Exarhos, G., and Moussas, X. (2010). Study of the solar slow sonic, Alfvén and fast magnetosonic transition surfaces. *Adv. Space Res.* 46, 382–390. doi: 10.1016/j.asr.2010.05.003

Kosovichev, A. G. (1996). Tomographic imaging of the Sun's interior. *Astrophys. J. Lett.* 461:L55. doi: 10.1086/309989

Kosovichev, A. G., Schou, J., Scherrer, P. H., Bogart, R. S., Bush, R. I., Hoeksema, J. T., et al. (1997). Structure and rotation of the solar interior: initial results from the MDI Medium-L program. *Solar Phys.* 170, 43–61. doi: 10.1023/A:1004949311268

Kosugi, T., Makishima, K., Murakami, T., Sakao, T., Dotani, T., Inda, M., et al. (1991). The Hard X-ray Telescope (HXT) for the SOLAR-A mission. *Solar Phys.* 136, 17–36. doi: 10.1007/BF00151693

Kramar, M., Airapetian, V., and Lin, H. (2016). 3D Global coronal density structure and associated magnetic field near solar maximum. *Front. Astron. Space Sci.* 3:25. doi: 10.3389/fspas.2016.00025

Kramar, M., Inhester, B., and Solanki, S. K. (2006). Vector tomography for the coronal magnetic field. I. Longitudinal Zeeman effect measurements. *Astron. Astrophys.* 456, 665–673. doi: 10.1051/0004-6361:20064865

Lavraud, B., Liu, Y., Segura, K., He, J., Qin, G., Temmer, M., et al. (2016). A small mission concept to the Sun-Earth Lagrangian L5 point for innovative solar, heliospheric and space weather science. *J. Atmos. Solar-Terrestr. Phys.* 146, 171–185. doi: 10.1016/j.jastp.2016.06.004

Leinert, C., Richter, I., Pitz, E., and Planck, B. (1981). The zodiacal light from 1.0 to 0.3 A.U. as observed by the Helios space probes. *Astron. Astrophys.* 103, 177–188.

Liewer, P. C., Alexander, D., Ayon, J., Kosovichev, A., Mewaldt, R., Socker, D., et al. (2009). "Solar Polar Imager: observing solar activity from a new perspective," in *NASA Space Science Vision Missions, Vol. 224*, ed M. S. Allen (Reston, VA: American Institute of Aeronautics and Astronautics), 1.

Liewer, P. C., Qiu, J., and Lindsey, C. (2017). Comparison of helioseismic far-side active region detections with STEREO far-side EUV observations of solar activity. *Solar Phys.* 292:146. doi: 10.1007/s11207-017-1159-3

Lindsey, C. and Braun, D. C. (1997). Helioseismic holography. *Astrophys. J.* 485, 895–903. doi: 10.1086/304445

Linker, J. A., Caplan, R. M., Downs, C., Riley, P., Mikic, Z., Lionello, R., et al. (2017). The open flux problem. *Astrophys. J.* 848:70. doi: 10.3847/1538-4357/aa8a70

Löptien, B., Birch, A. C., Gizon, L., Schou, J., Appourchaux, T., Blanco Rodríguez, J., et al. (2015). Helioseismology with Solar Orbiter. *Space Sci. Rev.* 196, 251–283. doi: 10.1007/s11214-014-0065-3

Lugaz, N., Temmer, M., Wang, Y., and Farrugia, C. J. (2017). The interaction of successive coronal mass ejections: A review. *Solar Phys.* 292:64. doi: 10.1007/s11207-017-1091-6

Mackay, D. H., and Yeates, A. R. (2012). The Sun's global photospheric and coronal magnetic fields: observations and models. *Living Rev. Solar Phys.* 9:6. doi: 10.12942/lrsp-2012-6

Mackay, D. H., Yeates, A. R., and Bocquet, F.-X. (2016). Impact of an L5 magnetograph on nonpotential solar global magnetic field modeling. *Astrophys. J.* 825:131. doi: 10.3847/0004-637X/825/2/131

Malanushenko, A., Schrijver, C. J., DeRosa, M. L., and Wheatland, M. S. (2014). Using coronal loops to reconstruct the magnetic field of an active region before and after a major flare. *APJ* 783:102. doi: 10.1088/0004-637X/783/2/102

McComas, D. J., Bame, S. J., Barraclough, B. L., Feldman, W. C., Funsten, H. O., Gosling, J. T., et al. (1998). Ulysses' return to the slow solar wind. *Geophys. Res. Lett.* 25, 1–4. doi: 10.1029/97GL03444

McComas, D. J., Elliott, H. A., Schwadron, N. A., Gosling, J. T., Skoug, R. M., and Goldstein, B. E. (2003). The three-dimensional solar wind around solar maximum. *Geophys. Res. Lett.*. 30:1517. doi: 10.1029/2003GL017136

McDonald, F. B., Trainor, J. H., Lal, N., Van Hollebeke, M. A. I., and Webber, W. R. (1977). Observations of galactic cosmic-ray energy spectra between 1 and 9 AU. *Astrophys. J.* 216, 930–939. doi: 10.1086/155537

McIntosh, P. S. (2003). "Patterns and dynamics of solar magnetic fields and HeI coronal holes in cycle 23," in *Solar Variability as an Input to the Earth's Environment. International Solar Cycle Studies (ISCS) Symposium* (Noordwijk), 807.

McIntosh, P. S., Krieger, A. S., Nolte, J. T., and Vaiana, G. (1976). Association of X-ray arches with chromospheric neutral lines. *Solar Phys.* 49, 57–77. doi: 10.1007/BF00221485

McIntosh, S. W., Davey, A. R., and Hassler, D. M. (2006). Simple magnetic flux balance as an indicator of Ne VIII Doppler velocity partitioning in an equatorial coronal hole. *Astrophys. J. Lett.*. 644, L87–L91. doi: 10.1086/505488

McIntosh, S. W., Leamon, R. J., Krista, L. D., Title, A. M., Hudson, H. S., Riley, P., et al. (2015). The solar magnetic activity band interaction and instabilities that shape quasi-periodic variability. *Nat. Commun.* 6:6491. doi: 10.1038/ncomms7491

Miesch, M. S. (2005). Large-scale dynamics of the convection zone and tachocline. *Living Rev. Solar Phys.* 2:1. doi: 10.12942/lrsp-2005-1

Müller, D., Marsden, R. G., St. Cyr, O. C., and Gilbert, H. R. (2013). Solar orbiter . Exploring the sun-heliosphere connection. *Solar Phys.* 285, 25–70. doi: 10.1007/s11207-012-0085-7

Neugebauer, M., Gloeckler, G., Gosling, J. T., Rees, A., Skoug, R., Goldstein, B. E., et al. (2007). Encounter of the Ulysses spacecraft with the ion tail of comet McNaught. *Astrophys. J.* 667, 1262–1266. doi: 10.1086/521019

Newmark, J. (2018). AGU meeting. *TESS Conference (21-24 May 2018)*.

Olmedo, O., Vourlidas, A., Zhang, J., and Cheng, X. (2012). Secondary waves and/or the "Reflection" from and "Transmission" through a coronal hole of an extreme ultraviolet wave associated with the 2011 February 15 X2.2 flare observed with SDO/AIA and STEREO/EUVI. *Astrophys. J.* 756:143. doi: 10.1088/0004-637X/756/2/143

Patsourakos, S., Georgoulis, M. K., Vourlidas, A., Nindos, A., Sarris, T., Anagnostopoulos, G., et al. (2016). The major geoeffective solar eruptions of 2012 March 7: comprehensive Sun-to-Earth analysis. *Astrophys. J.* 817:14. doi: 10.3847/0004-637X/817/1/14

Petrie, G. J. D., and Low, B. C. (2005). The dynamical consequences of spontaneous current sheets in quiescent prominences. *Astrophys. J. Supp. Ser.* 159, 288–313. doi: 10.1086/431149

Pevtsov, A. A., Bertello, L., MacNeice, P., and Petrie, G. (2016). What if we had a magnetograph at Lagrangian L5?. *Space Weather* 14, 1026–1031. doi: 10.1002/2016SW001471

Rieutord, M., and Rincon, F. (2010). The Sun's supergranulation. *Living Rev. Solar Phys.* 7:2. doi: 10.12942/lrsp-2010-2

Riley, P., Ben-Nun, M., Linker, J. A., Mikic, Z., Svalgaard, L., Harvey, J., et al. (2014). A multi-observatory inter-comparison of line-of-sight synoptic solar magnetograms. *Solar Phys.* 289, 769–792. doi: 10.1007/s11207-013-0353-1

Riley, P., Linker, J. A., Lionello, R., and Mikic, Z. (2012). Corotating interaction regions during the recent solar minimum: the power and limitations of global MHD modeling. *J. Atmos. Solar Terrest. Phys.* 83, 1–10. doi: 10.1016/j.jastp.2011.12.013

Robbrecht, E., Patsourakos, S., and Vourlidas, A. (2009). No trace left behind: STEREO observation of a coronal mass ejection without low coronal signatures. *Astrophys. J.* 701, 283–291. doi: 10.1088/0004-637X/701/1/283

Rosenbauer, H., Schwenn, R., Marsch, E., Meyer, B., Miggenrieder, H., Montgomery, M. D., et al. (1977). A survey on initial results of the Helios plasma experiment. *J. Geophys.* 42, 561–580.

Rouillard, A. P., Savani, N. P., Davies, J. A., Lavraud, B., Forsyth, R. J., Morley, S. K., et al. (2009). A multispacecraft analysis of a small-scale transient entrained by solar wind streams. *Solar Phys.* 256, 307–326. doi: 10.1007/s11207-009-9329-6

Sachdeva, N., Subramanian, P., Vourlidas, A., and Bothmer, V. (2017). CME dynamics using STEREO and LASCO observations: the relative importance of Lorentz forces and solar wind drag. *Solar Phys.* 292:118. doi: 10.1007/s11207-017-1137-9

Savani, N. P., Vourlidas, A., Pulkkinen, A., Nieves-Chinchilla, T., Lavraud, B., and Owens, M. J. (2013). Tracking the momentum flux of a CME and quantifying its influence on geomagnetically induced currents at Earth. *Space Weather* 11, 245–261. doi: 10.1002/swe.20038

Savani, N. P., Vourlidas, A., Richardson, I. G., Szabo, A., Thompson, B. J., Pulkkinen, A., et al. (2017). Predicting the magnetic vectors within coronal mass ejections arriving at Earth: 2. Geomagnetic response. *Space Weather* 15, 441–461. doi: 10.1002/2016SW001458

Savani, N. P., Vourlidas, A., Szabo, A., Mays, M. L., Richardson, I. G., Thompson, B. J., et al. (2015). Predicting the magnetic vectors within coronal mass ejections arriving at Earth: 1. Initial architecture. *Space Weather* 13, 374–385. doi: 10.1002/2015SW001171

Savcheva, A., McKillop, S., Hanson, E., McCauly, P., and DeLuca, E. (2014). Observed properties of sigmoidal regions and sigmoid evolutionary histories. *Solar Phys.* 289, 3297–3311.

Schou, J., and Bogart, R. S. (1998). Flows and horizontal displacements from ring diagrams. *Astrophys. J. Lett.* 504, L131–L134. doi: 10.1086/311575

Schrijver, C., and De Rosa, M. (2003). Photospheric and heliospheric magnetic fields. *Solar Phys.* 212:165. doi: 10.1023/A:1022908504100

Schrijver, C. J., and Title, A. M. (2011). Long-range magnetic couplings between solar flares and coronal mass ejections observed by SDO and STEREO. *J. Geophys. Res.* 116:A04108. doi: 10.1029/2010JA016224

Sekii, T., Appourchaux, T., Fleck, B., and Turck-Chièze, S. (2015). Future mission concepts for helioseismology. *Space Sci. Rev.* 196, 285–302. doi: 10.1007/s11214-015-0142-2

Semel, M., and Skumanich, A. (1998). An ambiguity-free determination of J_z in solar active regions. *Astron. Astrophys.* 331, 383–391.

Shapiro, A. I., Solanki, S. K., Krivova, N. A., Schmutz, W. K., Ball, W. T., Knaack, R., et al. (2014). Variability of Sun-like stars: reproducing observed photometric trends. *Astron. Astrophys.* 569:A38. doi: 10.1051/0004-6361/201323086

Shapiro, A. I., Solanki, S. K., Krivova, N. A., Yeo, K. L., and Schmutz, W. K. (2016). Are solar brightness variations faculae- or spot-dominated?. *Astron. Astrophys.* 589:A46. doi: 10.1051/0004-6361/201527527

Sheeley, N. R. Jr, Herbst, A. D., Palatchi, C. A., Wang, Y.-M., Howard, R. A., Moses, J. D., et al. (2008). SECCHI observations of the Sun's garden-hose density spiral. *Astrophys. J. Lett.* 674:L109. doi: 10.1086/529020

Solomon, S. C., McNutt, R. L., Gold, R. E., Acuña, M. H., Baker, D. N., Boynton, W. V., et al. (2001). The MESSENGER mission to Mercury: scientific objectives and implementation. *Planet. Space Sci.* 49, 1445–1465. doi: 10.1016/S0032-0633(01)00085-X

Tasnim, S., and Cairns, I. H. (2016). An equatorial solar wind model with angular momentum conservation and nonradial magnetic fields and flow velocities at an inner boundary. *J. Geophys. Res.* 121, 4966–4984. doi: 10.1002/2016JA022725

Thernisien, A., Vourlidas, A., and Howard, R. A. (2009). Forward modeling of coronal mass ejections using STEREO/SECCHI data. *Solar Phys.* 256, 111–130. doi: 10.1007/s11207-009-9346-5

Thompson, B. J., and Myers, D. C. (2009). A catalog of coronal "EIT Wave" transients. *Astrophys. J. Supp.* 183, 225–243. doi: 10.1088/0067-0049/183/2/225

Thompson, M. J., Christensen-Dalsgaard, J., Miesch, M. S., and Toomre, J. (2003). The internal rotation of the Sun. *Ann. Rev. Astron. Astrophys.* 41, 599–643. doi: 10.1146/annurev.astro.41.011802.094848

Thompson, W. T. (2006). Coordinate systems for solar image data. *Astron. Astrophys.* 449, 791–803. doi: 10.1051/0004-6361:20054262

Titov, V. S., Mikic, Z., Török, T., Linker, J. A., and Panasenco, O. (2012). 2010 August 1-2 sympathetic eruptions. I. Magnetic topology of the source-surface background field. *Astrophys. J.* 759:70. doi: 10.1088/0004-637X/759/1/70

Titov, V. S., Mikić, Z., Török, T., Linker, J. A., and Panasenco, O. (2017). 2010 August 1-2 sympathetic eruptions. II. Magnetic topology of the MHD background field. *Astrophys. J.* 845:141. doi: 10.3847/1538-4357/aa81ce

Tóth, G., Sokolov, I. V., Gombosi, T. I., Chesney, D. R., Clauer, C. R., de Zeeuw, D. L., et al. (2005). Space weather modeling framework: a new tool for the space science community. *J. Geophys. Res.* 110:A12226. doi: 10.1029/2005JA011126

Trichas, M., Gibbs, M., Harrison, R., Green, L., Eastwood, J., Bentley, B., et al. (2015). Carrington-L5: the UK/US operational space weather monitoring mission. *Hipparchos* 2, 25–31. Available online at: http://adsabs.harvard.edu/abs/2015Hipp....2l..25T

Tsuneta, S., Ichimoto, K., Katsukawa, Y., Lites, B. W., Matsuzaki, K., Nagata, S., et al. (2008). The magnetic landscape of the Sun's polar region. *Astrophys. J.* 688, 1374-1381. doi: 10.1086/592226

Ugarte-Urra, I., Upton, L., Warren, H. P., and Hathaway, D. H. (2015). Magnetic flux transport and the long-term evolution of solar active regions. *Astrophys. J.* 815:90. doi: 10.1088/0004-637X/815/2/90

Vasquez, A., Huang, Z., Manchester, W. B., and Frazin, R. A. (2011). The WHI corona from differential emission measure tomography. *Solar Phys.* 274, 259–284. doi: 10.1007/s11207-010-9706-1

Verdini, A., Velli, M., and Buchlin, E. (2009). Turbulence in the sub-Alfvénic solar wind driven by reflection of low-frequency alfvén waves. *Astrophys. J. Lett.* 700, L39–L42. doi: 10.1088/0004-637X/700/1/L39

Vourlidas, A. (2015). Mission to the Sun-Earth L_5 lagrangian point: an optimal platform for space weather research. *Space Weather* 13, 197–201. doi: 10.1002/2015SW001173

Vourlidas, A. (2017). "Solar Polar Diamond Explorer (SPDEx): understanding the origins of solar activity using a new perspective," in *White Paper Submitted* *in Response to Ideas for the Next Generation Solar Physics Mission Concepts*. Available online at: https://arxiv.org/abs/1805.04172

Wang, Y., Shen, C., Wang, S., and Ye, P. (2004). Deflection of coronal mass ejection in the interplanetary medium. *Solar Phys.* 222, 329–343. doi: 10.1023/B:SOLA.0000043576.21942.aa

Wang, Y.-M., and Sheeley, N. R. J. (1990). Solar wind speed and coronal flux-tube expansion. *Astrophys. J.* 355:726.

Webb, D. F., Biesecker, D. A., Gopalswamy, N., St. Cyr, O. C., Davila, J. M., Thompson, B. J., et al. (2010). Using STEREO-B as an L5 space weather pathfinder mission. *Space Res. Today* 178:10. doi: 10.1016/j.srt.2010.07.004

Webb, D. F., Gibson, S. E., Hewins, I. M., McFadden, R. H., Emery, B. A., Malanushenko, A., et al. (2018). Global solar magnetic field evolution over 4 solar cycles: use of the Mcintosh Archive. *Front. Astron. Space Sci.* 5:23. doi: 10.3389/fspas.2018.00023

Wilson, O. C. (1978). Chromospheric variations in main-sequence stars. *Astrophys. J.* 226, 379–396. doi: 10.1086/156618

Worden, J., and Harvey, J. (2000). An evolving synoptic magnetic flux map and implications for the distribution of photospheric magnetic flux. *Solar Phys.* 195, 247–268. doi: 10.1023/A:1005272502885

Wraight, K. T., White, G. J., Bewsher, D., and Norton, A. J. (2011). STEREO observations of stars and the search for exoplanets. *Month. Not. R. Astron. Soc.* 416, 2477–2493. doi: 10.1111/j.1365-2966.2011.18599.x

Xiong, M., and Liu, Y. (2014). in Taikong,ISSI-BJ magazine, volume 4.

Zhao, X. P., and Hoeksema, J. T. (2010). The magnetic field at the inner boundary of the heliosphere around solar minimum. *Solar Phys.* 266, 379–390. doi: 10.1007/s11207-010-9618-0

Conflict of Interest Statement: The authors declare that the research was conducted in the absence of any commercial or financial relationships that could be construed as a potential conflict of interest.